Transport in Porous Media 5: 103–151, 1990.

The Effect of Pore-Structure on Hysteresis in Relative Permeability and Capillary Pressure: Pore-Level Modeling

G. R. JERAULD and S. J. SALTER
Arco Oil & Gas Company, Research and Technical Services Plano, Texas, U.S.A.

(Received: 21 June 1988; revised: 26 May 1989)

Abstract. The effect of pore-structure upon two-phase relative permeability and capillary pressure of strongly-wetting systems at low capillary number is simulated. A pore-level model consisting of a network of pore-bodies interconnected by pore-throats is used to calculate scanning loops of hysteresis between primary drainage, imbibition and secondary drainage. The pore-body to pore-throat aspect ratio strongly influences the pattern of hysteresis. Changes in the patterns of hysteresis often attributed to consolidation can be understood in terms of changes in aspect ratio. Correlation between the sizes of neighboring pore-throats affects the shape of the relative permeability curves, while the width and shape of the pore-size distribution have only a minor influence.

Key words: Relative permeability, capillary pressure, hysteresis, pore-level modeling, pore-structure, network model, percolation theory.

1. Nomenclature

C	constant used in choke-off criterion
$f_b(r)$	probability density function for pore-bodies
$f_t(r)$	probability density function for pore-throats
g	hydraulic conductance associated with a pore-throat
H	mean curvature of the interface
k	absolute permeability
k_{rnwPD}	relative permeability of nonwetting phase in primary drainage
k_{rnwIM}	relative permeability of nonwetting phase in imbibition
k_{rnwSD}	relative permeability of nonwetting phase in secondary drainage
k_{rwPD}	relative permeability of wetting phase in primary drainage
k_{rwIM}	relative permeability of wetting phase in imbibition
k_{rwSW}	relative permeability of wetting phase in secondary drainage
l	length of pore-throat (idealized as a capillary)
N_{ca}	capillary number
p_i	pressure in phase i
P_c	capillary pressure
q	total fluid flow through a pore-throat
r_b	pore-body radius
r_t	pore-throat radius

R_1, R_2	the radii of curvature along interface
S_b	volume fraction of pore-bodies occupied by nonwetting phase
S_{nw}	saturation of nonwetting phase
S_t	volume fraction of the pore-throats occupied by nonwetting phase
S_w	saturation of wetting phase
$\mathbf{u}_i$	velocity of phase i
x	fraction of the pore-space taken up by pore-throats
z	coordination number, i.e. number of pore-throats emanating from a pore-body
z_{nw}	number of pore-throats filled with nonwetting phase adjoining a pore-body
μ_i	viscosity of phase i
σ	interfacial tension
Ω_b	random number assigned to pore-body used for assigning pore-body radius
Ω_t	random number assigned to pore-throat used for assigning pore-throat radius

2. Introduction

Relative permeability and capillary pressure are used to predict the relative rates at which fluids flow through porous media, and therefore, are essential ingredients in the design of petroleum recovery processes and the prediction of groundwater flow. Complicated flow histories make knowledge of hysteresis behavior necessary for accurate process design. Design of processes which are stable with respect to viscous fingering requires accurate estimates of relative permeability. Hysteresis in capillary pressure and relative permeability impact well coning behavior (Killough, 1976), the prediction of gas storage in aquifers (Evrenos and Comer, 1969), redistribution of water after initial infiltration (Talsma, 1970), the rate of solute transport in ground water flow, the amount of phases disconnected during a displacement (Pickell *et al.*, 1966; Land, 1968; Keelan and Pugh, 1975; Wardlaw and Taylor, 1976) and the origin of unusual frontal behavior (Gladfelter and Gupta, 1978). Empirical models of relative permeability incorporating hysteresis into numerical simulators have been described by a number of people (c.f. Land, 1968; Evrenos and Comer, 1969; Colonna and Millet, 1970; Killough, 1976; Aziz and Settari, 1979; Ramakrishnan and Wasan, 1986).

This paper examines the effect of pore-structure on patterns of relative permeability and capillary pressure hysteresis which occur in two-phase, low capillary number flow of strongly-wetting fluids. It is intended to provide physical explanations of hysteresis along with a mechanistic model for predicting the effects of rock structure. We begin with the basic concepts which delineate the subject and scope of our study.

2.1. PRELIMINARIES

The concepts of relative permeability and capillary pressure are well-defined for the slow flow of immiscible fluids through a porous medium. The flow rate per unit area of porous medium of a phase i, $\mathbf{u}_i$, is related to the pressure gradient in that phase, ∇p_i, through the generalized Darcy's law:

$$\mathbf{u}_i = -\frac{kk_{ri}}{\mu_i}\nabla p_i,$$

where k is absolute permeability, μ_i is the viscosity of phase i, and k_{ri} is the relative permeability of phase i. Relative permeability accounts for the reduction of permeability to a phase created when it does not fully occupy the porous medium. Hence, the relative permeability of a phase is usually taken to be unity when the phase fully occupies the medium and is zero when the volume fraction of the pore-space that a phase occupies, its *saturation*, is sufficiently low; this saturation is called the irreducible or *residual saturation*. Sufficient conditions for the concept of relative permeability to apply are that the flow is sufficiently slow that capillary forces dominate viscous forces and that the saturation gradients are small, i.e. saturation does not change appreciably over a distance of >20 pores (e.g. >1 mm in Berea sandstone). These conditions are typically applicable during steady-state relative permeability measurements.

Capillary pressure is the equilibrium pressure difference between the nonwetting and wetting phases (Adamson, 1982)

$$P_c \equiv p_{\mathrm{nw}} - p_{\mathrm{w}}$$

Differential movement of the fluids within a porous medium can result from gradients in capillary pressure, relative permeability effects, and also density differences.

The analysis below pertains to strongly-wetting fluids, i.e. ones in which the contact angle between the wetting and nonwetting fluids on the solid comprising the porous medium is less than 30° (for summary, see Anderson, 1986, 1987); for simplicity we have assumed that the contact angle is strictly zero. Many interesting systems do not satisfy these criteria (e.g. mixed-wet and intermediate-wet systems). While wettability effects can create their own set of hysteresis phenomena, they are outside the scope of the work to be described here.

A criterion often used to judge whether flow of strongly-wetting fluids is capillarity dominated (Moore and Slobod, 1956; Tabor, 1969; Melrose and Bradner, 1976) is that the capillary number

$$N_{\mathrm{ca}} \equiv \frac{k\|\nabla p\|}{\sigma} < 10^{-5},$$

where σ is the interfacial tension and ∇p is the gradient in the pressure field (maximum of that in the wetting and nonwetting phases). Many people have shown

experimentally that relative permeability and capillary pressure are independent of flow rate when the flow is sufficiently slow to satisfy this criterion (c.f. Osoba *et al.*, 1951; Richardson *et al.*, 1952; Sandberg *et al.*, 1958; Labastie *et al.*, 1980). The work presented here is applicable only to cases of capillarity dominated flow.

Relative permeability depends primarily upon the microscopic distribution of the fluids within the pore space. Under low capillary number conditions, the distribution of fluids at the pore scale is determined by capillary forces and depends upon the level of saturation, the saturation history and direction of saturation change. The dependence of flow upon the sequence in which phases are introduced, or saturation history, and the direction of saturation change is called *hysteresis*, the major topic of this paper. We consider here, a sequence of fluid displacements in which the wetting fluid initially resides in the porous medium. The processes which follow are:

(1) *primary drainage* in which nonwetting fluid first displaces the wetting fluid, thus decreasing the wetting phase saturation,
(2) *imbibition* (secondary) in which wetting fluid is added to increase the wetting phase saturation, and
(3) *secondary drainage* in which nonwetting fluid again displaces wetting fluid from the medium.

Scanning loops are formed by varying the saturation achieved during drainage before imbibition.

A number of researchers have measured hysteresis in relative permeability and capillary pressure and have determined that the patterns of hysteresis can be related to pore-structure. Much of the previous effort has been devoted to understanding differences between consolidated and unconsolidated media, especially between sand and sandstone. Because of the variety of pore-structures which occur naturally and difficulties inherent in measuring relative permeability, it is difficult to infer anything but an over-simplified picture of how relative permeability curves change with pore-structure from experimental data. We therefore developed the pore-level model so that a more direct cause and effect relationship could be derived between pore structure and relative permeability. A pattern of relative permeability behavior distilled from the literature is as follows.

2.2. EXPERIMENTALLY OBSERVED PATTERNS OF HYSTERESIS BEHAVIOR

Examples of the variety of experimentally observed hysteresis patterns appear in Figure 1. In almost all capillary-dominated flows of strongly-wetting phases, the nonwetting phase relative permeability shows much more hysteresis than the wetting phase. In consolidated media, like sandstone, the nonwetting phase relative permeability in primary drainage (k_{rnwPD}) is greater than that in imbibition (k_{rnwIM}), while k_{rnwIM} is roughly the same as that in secondary drainage (k_{rnwSD}). In unconsolidated media, like sand or beadpacks, the nonwetting phase relative

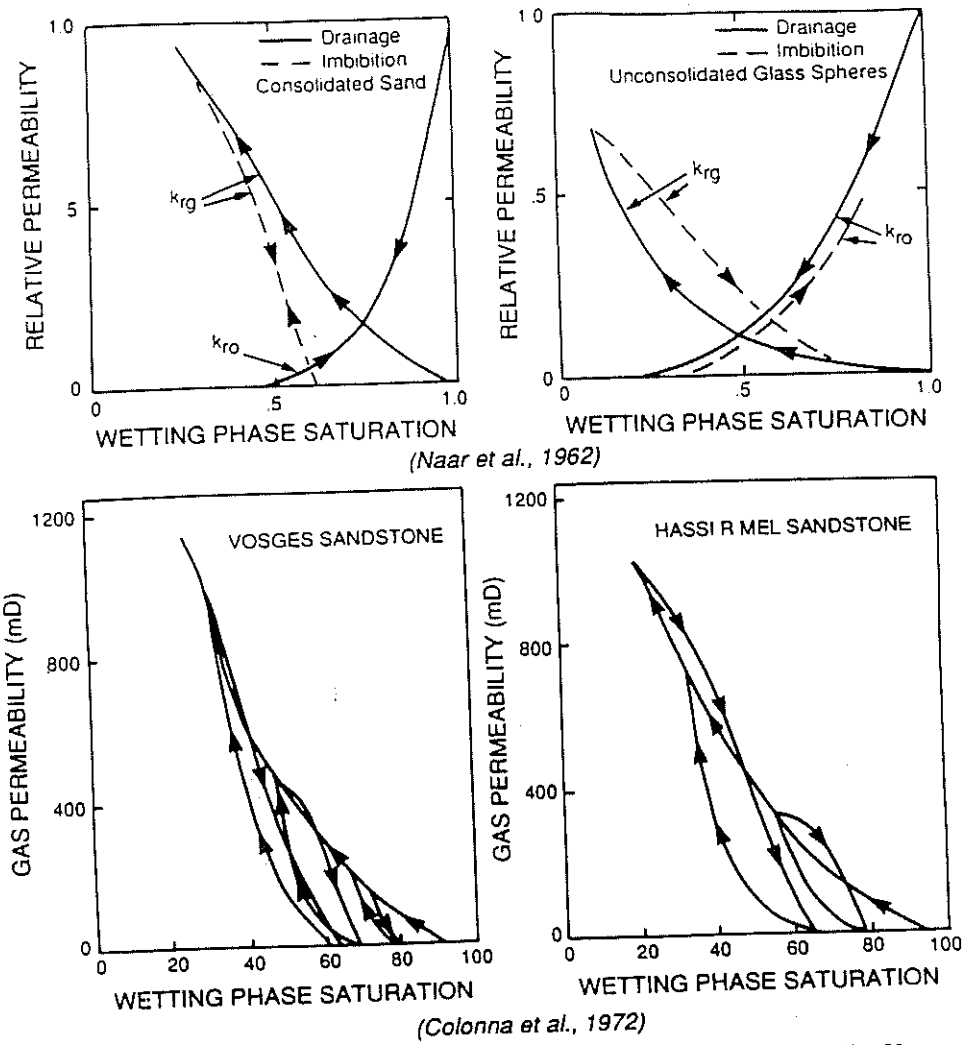

Fig. 1. Patterns of hysteresis in relative permeability for strongly-wetting porous media. Upper – pattern for consolidated sandstone (left) and unconsolidated glass spheres (right) after Naar *et al.* (1962). Lower – patterns for nonwetting phase relative permeability, after Colonna *et al.* (1972).

permeability is greater in imbitition than in primary drainage, while that in secondary drainage is roughly the same as that in primary drainage. Consolidated media have higher residual nonwetting phases (in imbibition) than unconsolidated media. Although hysteresis in wetting phase relative permeability is often considered negligible compared to the uncertainty of the measurements, both larger and smaller values in drainage, as compared to imbibition, have been reported for both consolidated and unconsolidated media. In summary

$$\text{consolidated media: } k_{rnw}^{PD} \geq k_{rnw}^{IM} \approx k_{rnw}^{SD};\ k_{rw}^{PD} \approx k_{rw}^{IM} \approx k_{rw}^{SD},$$

$$\text{unconsolidated media: } k_{rnw}^{IM} > k_{rnw}^{PD} \approx k_{rnw}^{SD};\ k_{rw}^{PD} \approx k_{rw}^{IM} \approx k_{rw}^{SD}.$$

Representative data showing the difference between the drainage and imbibition relative permeability in media of different degrees of consolidation is given in Figure 1 (Naar *et al.*, 1962). A partial list of trends reported in the literature for consolidated and unconsolidated media appears in Table I.

Colonna *et al.* (1971) report patterns of hysteresis in nonwetting phase relative permeability which are in marked contrast to those presented by Naar *et al.* (1962) (Figure 1 shows a comparison). They measured relative permeability of gas, including hysteresis loops, in two different sandstones and found that $k_{rnw^{IM}}$ was greater than $k_{rnw^{PD}}$ at low wetting phase saturations, then crossed over and was less than $k_{rnw^{PD}}$ at high wetting phase saturations. $k_{rnw^{SD}}$ was smaller than $k_{rnw^{IM}}$ and $k_{rnw^{PD}}$ at high wetting phase saturations and eventually rejoined the primary drainage relative permeability curve at sufficiently high wetting phase saturations.

Table I. Summary of relative permeability hysteresis patterns for strongly-wetting systems reported in the literature.

Porous media	Nonwetting phase	Wetting phase	Reference
Consolidated sandstone	$k_{rnw^{IM}} \leqslant k_{rnw^{PD}}$	$k_{rnw^{IM}} \geqslant k_{rw^{PD}}$ (small)	Osoba *et al.* (1951)
Consolidated limestone	$k_{rnw^{IM}} \leqslant k_{rnw^{PD}}$	$k_{rw^{IM}} \geqslant k_{rw^{PD}}$ (small)	Osoba *et al.* (1951)
Consolidated sandstone	$k_{rnw^{IM}} < k_{rnw^{PD}}$	$k_{rw^{IM}} \geqslant k_{rw^{PD}}$ (small)	Geffen *et al.* (1951)
Consolidated sandstone	$k_{rnw^{IM}} < k_{rnw^{PD}}$	$k_{rw^{IM}} \geqslant k_{rw^{PD}}$ (small)	Naar *et al.* (1962)
Poorly consolidated sandstone	$k_{rnw^{IM}} \leqslant k_{rnw^{PD}}$	$k_{rw^{IM}} < k_{rw^{PD}}$ (small)	Naar *et al.* (1962)
Berea sandstone	$k_{rnw^{IM}} \leqslant k_{rnw^{PD}}$		Ramondi and Torcaso (1964)
Berea sandstone	$k_{rnw^{IM}} < k_{rnw^{PD}}$	$k_{rw^{IM}} \approx k_{rw^{PD}}$ (small)	Talash (1976)
Berea sandstone	$k_{rnw^{IM}} \leqslant k_{rnw^{PD}}$	$k_{rw^{IM}} \leqslant k_{rw^{PD}}$ (small)	Fulcher *et al.* (1985)
Berea sandstone	$k_{rnw^{IM}} \approx k_{rnw^{SD}} < k_{rnw^{PD}}$	$k_{rw^{IM}} \approx k_{rw^{SD}} < k_{rw^{PD}}$	this work
Glass beads	$k_{rnw^{IM}} > k_{rnw^{PD}}$	$k_{rw^{IM}} < k_{rw^{PD}}$	Naar *et al.* (1962)
Sandpacks	$k_{rnw^{IM}} > k_{rnw^{SD}} \approx k_{rnw^{PD}}$	$k_{rw^{IM}} \leqslant k_{rw^{PD}} < k_{rw^{PD}}$ (small)	Batycky and McCaffery (1978)
Glass beads	$k_{rnw^{IM}} > k_{rnw^{PD}}$	$k_{rw^{IM}} \leqslant k_{rw^{SD}} < k_{rw^{PD}}$	Hopkins and Ng (1986)
Sandpack		$k_{rw^{IM}} < k_{rw^{SD}}$	Poulovassilis (1970)
Glass beads		$k_{rw^{IM}} \leqslant k_{rw^{SD}}$	Topp and Miller (1966)
Glass beads		$k_{rw^{IM}} \approx k_{rw^{SD}}$	Talsma (1970)

3. Foundations of Our Model

The exact flow field in a porous rock and the relative permeability of a phase can be calculated if the details of the pore structure are known and a large enough and fast enough computer exists. The laws that determine the flow are the traditional laws of fluid mechanics and capillarity. Such a calculation is, of course, prohibitively expensive and, in fact, unnecessary. The essential features of relative permeability can be understood and simulated by a network model. The general idea behind network models is to approximate the description of the pore-space and movement of fluids therein by a small set of parameters and simple rules governing the movement of fluids. Our work most closely builds upon the work of Mohanty and Salter (1982) and incorporates a number of new features.

In the next five sections we present the essence of our model, motivating our description of the pore-space and fluid flow within it. The assumptions which underlie the model are discussed thoroughly, with an attempt to explain the physical rationale behind each one. To understand our model, the reader first must understand the reduction of a porous medium to its network approximation. Second, one needs a description of the factors which determine the distribution of fluids within a porous medium. Flow within the medium occurs on two widely different timescales. One timescale is characteristic of the rapid progression between quasi-equilibrium configurations of the menisci (these pore-level events, which are the third element of our model, determine the microscopic fluid distribution). The procedure for calculating the fluid saturations determined by these pore-level events is the fourth element. The other timescale characterizes the flow of fluids through a given microscopic fluid distribution. And, thus the fifth element is the procedure for calculating relative permeability. Let us begin with a description of pore-space morphology.

3.1. PORE-SPACE MORPHOLOGY

Three major features characterize the morphology of the pore-space in our model: a network, pore-throat and pore-body size distributions. We have endeavored to use realistic parameters in the calculations presented below, but have neither attempted to measure these quantities ourselves, nor have we varied the parameters extensively to obtain a quantitative 'fit' of experimental data.

We approximate the porous medium as a network of spherical pore-bodies connected by cylindrical tubes. This network description is perhaps the simplest model that includes all the features necessary to understand the hysteresis behavior of relative permeability. Although the idea of a network dates back to a least Fatt (1956), methods of efficiently approximating the pore-space of a porous medium with a network are still under development. General schemes of reducing a pore-space to networks have been proposed by Chatzis and Dullien (1977), Chatzis (1980), Mohanty (1981), Cohen and Lin (1981), and Koplik (1982). These schemes have been further developed and augmented in attempts to use information from

serial sectioning and digitization to calculate pore-size distributions and transport properties (Koplik *et al.*, 1984; Yanuka *et al.*, 1984; Yanuka *et al.*, 1986; MacDonald *et al.*, 1986; Ruzyla, 1986).

Network structure entails a number of different features: *scale*, *dimensionality*, *coordination number* and *distribution of coordination*. In addition, distributions of pore-throat and pore-body sizes are required. In the following paragraphs we discuss the basis on which we have selected the values used in our calculations.

The *scale* of the network determines the distance between pore-bodies or, equivalently, the length of pore-throats. We have chosen this scale so that coupled with the pore-body and pore-throat radii, the porosity of the porous medium is correct. The scale of the network is also consistent with the approximate size of grains of sand in a sandstone or beads in a beadpack.

Although two-*dimensional* (2D) networks are less expensive and easier to work with, we believe it is important to use three-dimensional (3D) networks in modeling 3D flow behavior because there are more interconnections in 3D systems. The effects of interconnections are most pronounced in systems where the wetting phase is disconnected or trapped such as the invasion percolation model of displacement (Chandler *et al.*, 1982; Wilkinson and Willemson, 1983; Koplik *et al.*, 1983). When the invasion percolation model is formulated in 2D, only one phase can percolate across the system at a time; while in 3D, there is a range of saturations in which two-phases can flow (breakthrough of one phase corresponds to a residual of the other in 2D!). In addition, the residual to the nonwetting phase is much higher in a 2D system than in a 3D system. For a uniform distribution of pore-sizes, the residual to nonwetting phase may be over-estimated by as much as 1/3 by using a 2D network relative to a 3D network of the same coordination (Chatzis and Dullien, 1982). The exponents governing critical behavior in percolation theory are different in 2D and 3D indicating differences in scaling between 2D and 3D systems (Wilkinson, 1986). Because the wetting phase is not disconnected in our model, the wetting phase does not stop flowing but, instead, the relative permeability of the wetting phase decreases markedly when there is no longer an interconnected set (backbone) of pores completely filled of wetting fluid spanning the network. Hence, the differences between two and three dimensional systems will still be present in our model but will be less severe.

Measurements of *coordination number* (i.e. number of pore-throats emanating from a pore-body) reported in the literature vary depending upon the technique and the properties of the medium. For regular packings of spheres Yuan (1981) found that average coordination number of the pore-space, $\bar{z}$, was in the range $4 \leqslant \bar{z} \leqslant 8$, and inferred that sandstones tend to have lower coordination than sphere-packs; Berea sandstone would have an average coordination number of roughly 5 according to his estimates. Chatzis *et al.* (1983) studied the structure of the residual oil (nonweting phase) in Berea sandstone and found coordination numbers in the center of large blobs in the range of 3 to 8. Yanuka *et al.* (1985)

used serial sectioning and reported a coordination distribution for Berea sandstone which is sharply peaked around $z = 3$ with $\bar{z} = 2.8$, and for glass bead packs $\bar{z} = 4.3$. Their technique gave low estimates of the average coordination number for regular packings of known coordination. In addition, their reported distributions include large fractions of pores with coordination numbers of $z = 1$ and $z = 2$ which we do not consider as distinct pores – when these pores are taken out of their distributions, the average increases to 4.9 for Berea and 5.3 for a random bead pack. Lin and Cohen (1982) used serial sectioning techniques and measured $\bar{z} = 2.9$ for Berea sandstone as did Koplik *et al.* (1984) who also used serial sectioning and estimate $\bar{z} = 3.49$ for Massilon sandstone. These latter estimates also include some dead-end pores and pores of coordination 2. Based on all these reported data and model results, we conclude that coordination numbers between 4 and 8 are realistic.

In many of our studies we have used networks which have an average *coordination number* of six. We have studied both regular cubic networks and random Voronoi networks (Voronoi, 1908; Meijering, 1953; Winterfeld, 1981; Jerauld *et al.*, 1984). These Voronoi networks are generated by using the Voronoi construction to form space-filling polyhedra, replacing the polyhedra with pore-bodies centered at the polyhedra centroids, and substituting pore-throats connecting pore-bodies for each face of the polyhedra. The network formed has an average coordination number of approximately 15.54 which is large compared to that of the pore-space of natural media. We, therefore, reduce the average coordination of the network to 6 by discarding the pore-throats connecting pore-bodies which are furthest away from each other. The resulting networks have a distribution of coordination varying from 3 to 12.

In general, we find that results (relative permeability) for regular and random systems are nearly identical. Jerauld *et al.* (1984) found that the percolation properties (e.g. effective conductivity) were the same for Voronoi and regular networks, in both 2D and 3D, consistent with the results reported here for relative permeability. The magnitude of the coordination number does affect the results. For example, decreasing the coordination number increases the residual saturation and the capillary pressure at breakthrough for a given pore-size distribution (c.f. Chatzis and Dullien, 1982, 1984).

Pore-size distributions of rocks have been measured by many people using a variety of methods (Dullien and Dhawan, 1974, 1975; Chatzis and Dullien, 1982; Chatzis *et al.*, 1983; Yanuka *et al.*, 1986). Most methods require a model of the pore-space and simplifying assumptions. Because of these difficulties and the simplified model we use, we have not attempted to precisely determine pore-size distributions but use simple functional forms and sizes that roughly approximate those given in the literature. We have used two different distributions in the work presented below, one designed to mimic the properties of sandstone (Berea, Figure 2) and the other a monodisperse beadpack (Figure 3). The pore-size distribution we use for Berea is similar to that used by Chatzis and Dullien (1982) and has the

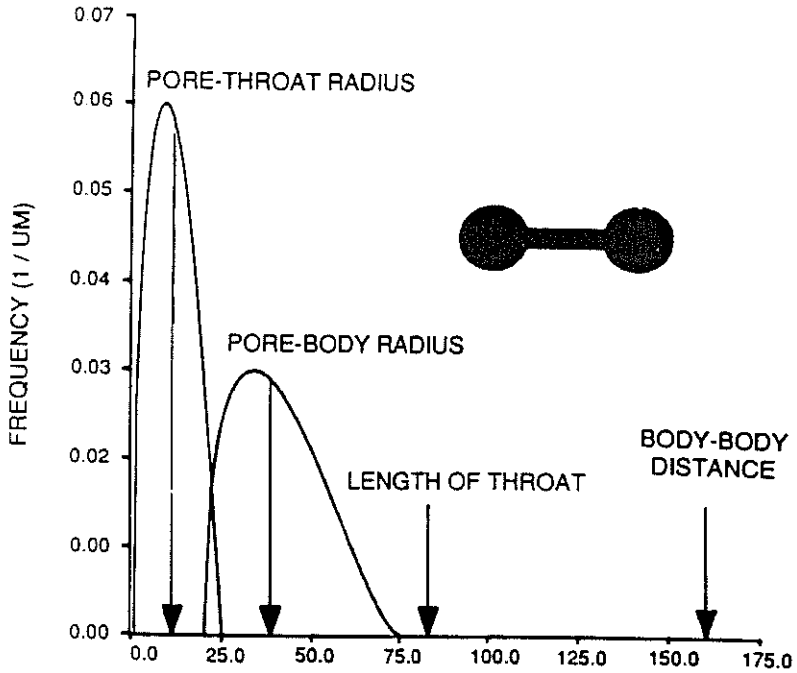

Fig. 2. Pore-size distribution representative of a consolidated porous medium (Berea sandstone). Pore-throats are somewhat smaller than pore-bodies; $\bar{r}_t = 11\ \mu$m, $\bar{r}_b = 38\ \mu$m, average body-body distance = 160 μm, average length of throat = 83 μm.

normalized probability density functions

$$f_t(r) = \frac{15}{4}\xi^{0.5}(1-\xi), \qquad f_b(r) \propto \xi^{0.25}(1-\xi)^{1.5}$$

where

$$\xi = \frac{(r - r^{\min})}{(r^{\max} - r^{\min})}$$

with

$$r_t^{\min} = 1\ \mu\text{m}, \quad r_t^{\max} = 25\ \mu\text{m}, \quad \bar{r}_t = 11\ \mu\text{m},$$
$$r_b^{\min} = 20\ \mu\text{m}, \quad r_b^{\max} = 75\ \mu\text{m}, \quad \bar{r}_b = 38\ \mu\text{m}.$$

The distance between the centers of pore-bodies is 160 μm. Our pore-size distribution for monodisperse spheres is similar to the one given by Payatakes *et al.* (1980) and is

$$f_t(r) \propto \xi^{0.50}(1-\xi)^{0.50}, \qquad f_b(r) \propto \xi^{1.50}(1-\xi)^{0.5}$$

with

$$r_t^{\min} = 15\ \mu\text{m}, \quad r_t^{\max} = 40\ \mu\text{m}, \quad \bar{r}_t = 27.5\ \mu\text{m},$$
$$r_b^{\min} = 40\ \mu\text{m}, \quad r_b^{\max} = 64\ \mu\text{m}, \quad \bar{r}_b = 56\ \mu\text{m}.$$

The distance between the centers of pore-bodies is 150 μm.

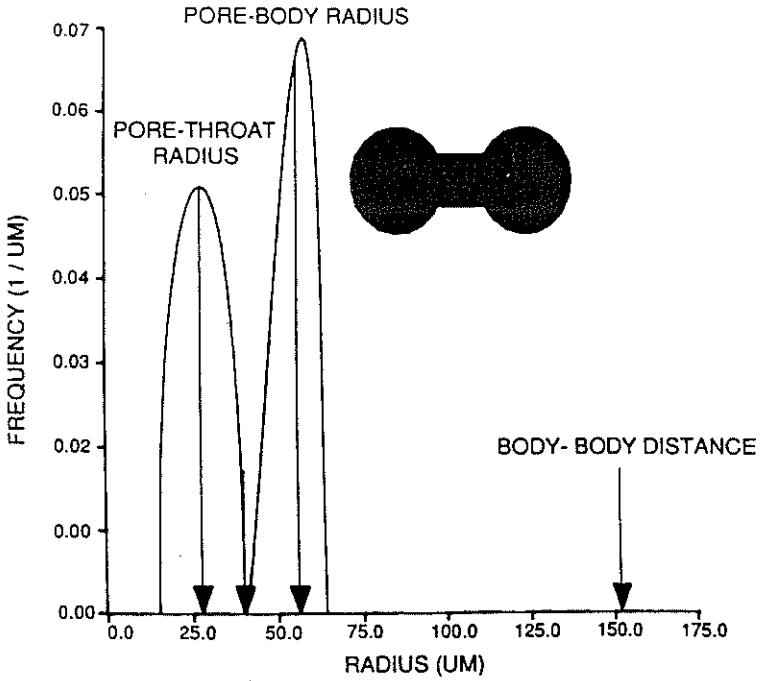

Fig. 3. Pore-size distribution representative of an unconsolidated porous medium (sphere-pack); $\bar{r}_t = 28\ \mu m$, $\bar{r}_b = 56\ \mu m$, average body-body distance = 152 μm, average length of throat = 40 μm.

3.2. FLUID DISTRIBUTION WITHIN THE PORE-SPACE

To effectively model the transport of the phases one must first know their microscopic distribution. The configuration of the wetting phase affects both the relative permeability and the amount of wetting phase present when the relative permeability is negligible, the apparent irreducible wetting phase saturation practically achievable in the laboratory. A number of researchers have provided evidence that in porous media with rough surfaces, the wetting phase exists as a connected network on the surface of the pore-space consisting of thin films and pendular structures. The irreducible wetting phase saturation is usually sufficiently large in natural porous media that it cannot be accounted for simply as adsorbed films, but exists as bulk phases in the surface grooves, nooks and crannies of the pore-walls (Morrow, 1970). Adsorbed films probably account for less than one saturation percent. Dullien *et al.* (1986) found that there seems to be no lower bound to the irreducible saturations of wetting phase in Berea cores (upon application of increasing amounts of pressure) and present SEM evidence that "the wetting phase present in the pore corners or edges forms a continuum . . . , a network of conduits throughout which trapped wetting phase can leak out and be produced". Russell *et al.* (1947), working with sandstone after displacement with oil (nonwetting phase), and Brown (1957), working in sandpacks, found that

all the water left after displacement with oil was recovered upon subsequent imbibition. Salter and Mohanty (1982) found no isolated wetting phase during two-phase steady-state flow over a wide range of saturations in fired and acidized Berea sandstone. Meyers and Salter (1983) found that all the ion exchange sites (and hence the entirety of the pore-walls) are accessible through the wetting phase in Berea sandstone partially saturated with oil. Bacri *et al.* (1985) measured the saturation profile formed when wetting fluid is injected at low rates into sandstone. They showed that if the sandstone was pre-wet with wetting fluid, the saturation will increase throughout the sample without forming a distinct front, indicating transport of wetting phase through thin films. However, if the solid was not pre-wet by the wetting phase, its saturation increases only at the saturation front that forms. A number of researchers have also found that even on relatively smooth surfaces, such as glass micromodels, the wetting phase remains hydraulically connected through microscopic grooves in the solid surface and the corners of pores with angular cross-section (Mattax and Kyte, 1961; Lenormand *et al.*, 1983; Lenormand and Zarcone, 1984; Mathers and Dawe, 1985; Dullien *et al.*, 1986). The relative permeability to the nonwetting phase at irreducible wetting phase saturation is often nearly unity (e.g. Leverett, 1938; Ramondi and Torasco, 1964; Morgan and Gordon, 1970; Muskat *et al.*, 1937), hence these surface grooves, nooks and crannies do not contribute much to the total permeability of the medium. Based on these observations, we assume that the wetting phase does not become disconnected and that the hydraulic conductance of a throat occupied with nonwetting phase is the same as in single phase flow.

3.3. PORE-LEVEL EVENTS

In flows at low capillary number, saturation fronts move through the porous medium via a sequence of interfacial jumps. These jumps occur over a much smaller timescale than typifies the bulk fluid movement. Such flows can be modelled as pseudostatic, in which the flow occurs as a sequence of essentially equilibrium configurations. The rules, or pore-level events, governing movement from one configuration to the next have been derived by a number of researchers and are based upon calculations of stability of interfaces in simple geometries and upon micromodel studies (Mattax and Kyte, 1961; Pickell *et al.*, 1966; Roof, 1970; Lenormand *et al.*, 1983; Chatzis *et al.*, 1983; Lenormand and Zarcone, 1984; Chen and Koplik, 1985; Li and Wardlaw, 1985; Mohanty *et al.*, 1987). The type of events which occur depends upon whether the process is drainage or imbibition, and the geometry of the pore-space. We describe all flows in terms of three pore-level events, which we characterize from the point of view of the nonwetting phase: (1) invasion, (2) choke-off, and (3) retraction.

For simplicity, we explain concepts in terms of a network of cylinders with 'throat radii', r_t, connected at spheres (or pore-bodies) of radius r_b. These radii

should be interpreted as the effective radii of curvature of the interfaces that fit inside the pore-bodies and pore-throats within the porous medium of interest.

In drainage, the capillary pressure begins at a low value and increases. The nonwetting phase saturation increases as nonwetting fluid invades successively smaller pores, and becomes connected to regions which were separated from this phase by small throats. A pore-throat is invaded if the applied capillary pressure is greater than that which can be withstood by an interface sitting in the pore-throat, i.e. if

$$P_c < 2H\sigma \equiv \left(\frac{1}{R_1} + \frac{1}{R_2}\right)\sigma \approx \frac{2\sigma}{r_t}$$

Here H represents the mean curvature of the interface, and R_1 and R_2 are the radii of curvature along the two principle axes. The last equality holds only for cylindrical pore-throats and may be regarded as the definition of an effective radius of curvature, with the added idea that it represents the smallest radius of curvature along the length of the pore-throat. Pore-bodies are assumed to be larger than pore-throats. Hence, after going through a pore-throat, an interface spontaneously invades the adjoining pore-body via a *Haines jump* as is depicted in Figure 4.

If the throat just passed is sufficiently small, the narrow neck meniscus left behind in the pore-throat may not be stable, and can collapse if the ratio of the pore-body radius to pore-throat radius is sufficiently large. As the drainage displacement proceeds, the pore-throat will be subsequently invaded again (Chen and Koplik, 1985). Because of this bubbling, these pore-throats allow transport of the nonwetting phase but may be closed to the nonwetting phase in the relative permeability calculation. The effect of this mechanism upon the relative permeability is however negligible and may be ignored. In primary drainage, the fluid begins along the exterior of the network and invades the largest pore-throat along the interface. At every step in the primary drainage process, nonwetting fluid resides in the pore-throats and bodies accessible through throats with a radius larger than that corresponding to the current capillary pressure. In secondary drainage, nonwetting phase can be present as that trapped in imbibition or that accessible to the exterior of the network.

Near the end of drainage processes, when the capillary pressure is high, the centers of virtually all of the pore-bodies and pore-throats are filled with nonwetting fluid. The remaining wetting phase is left in the form of thin films along the pore-walls, and pendular structures in the nooks and crannies. At capillary equilibrium, these films and pendular structures are thinner at higher capillary pressures, which reduces the wetting phase saturation at which flow stops. Because of its very low hydraulic conductance, the wetting phase may not reach its equilibrium saturation within the timescale of many experiments. This resistance to flow leads to the observation that irreducible water saturation depends upon how long

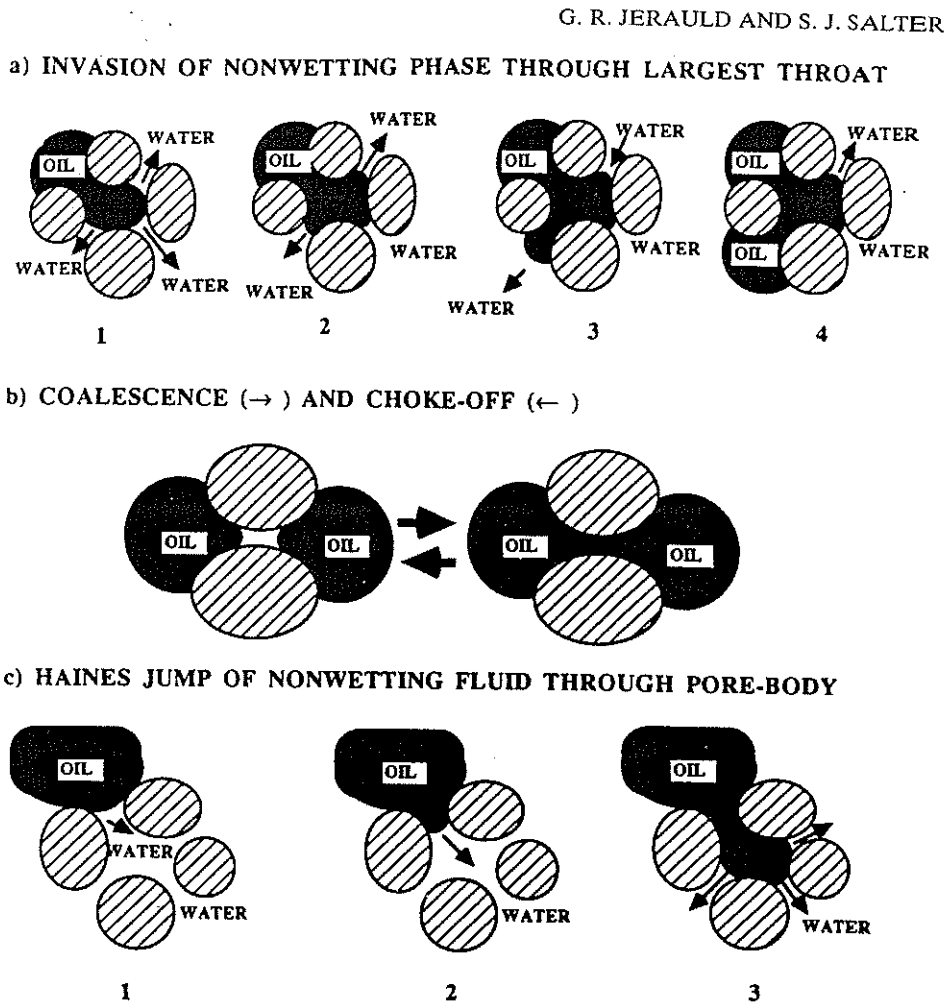

Fig. 4. Pore-level events in drainage. (a) Invasion of nonwetting phase (oil) through largest pore-throat, followed by (b) coalescence of nonwetting phase (if neighboring pore-body is filled with nonwetting phase) and possibly reverse, snap-off or (c) Haines jump through adjoining pore-body (if neighboring pore-body is filled with wetting phase).

the experimentalist is willing to wait. Proper consideration of these phenomena involves both an elaborate treatment of the surface forces, and a more accurate description of the geometry of the surface of the porous medium, and is beyond the scope of our current study.

In imbibition, the capillary pressure decreases from the value attained at the end of the primary drainage cycle. Nonwetting phase, which is accessible from the exterior of the network, is either displaced from small throats via *choke-off* (or *snap-off*, Figure 5) or displaced from small pore-bodies in an event called *retraction* (Figure 5). In choke-off, a solenoidal, or saddle-shaped, interface in a pore-throat

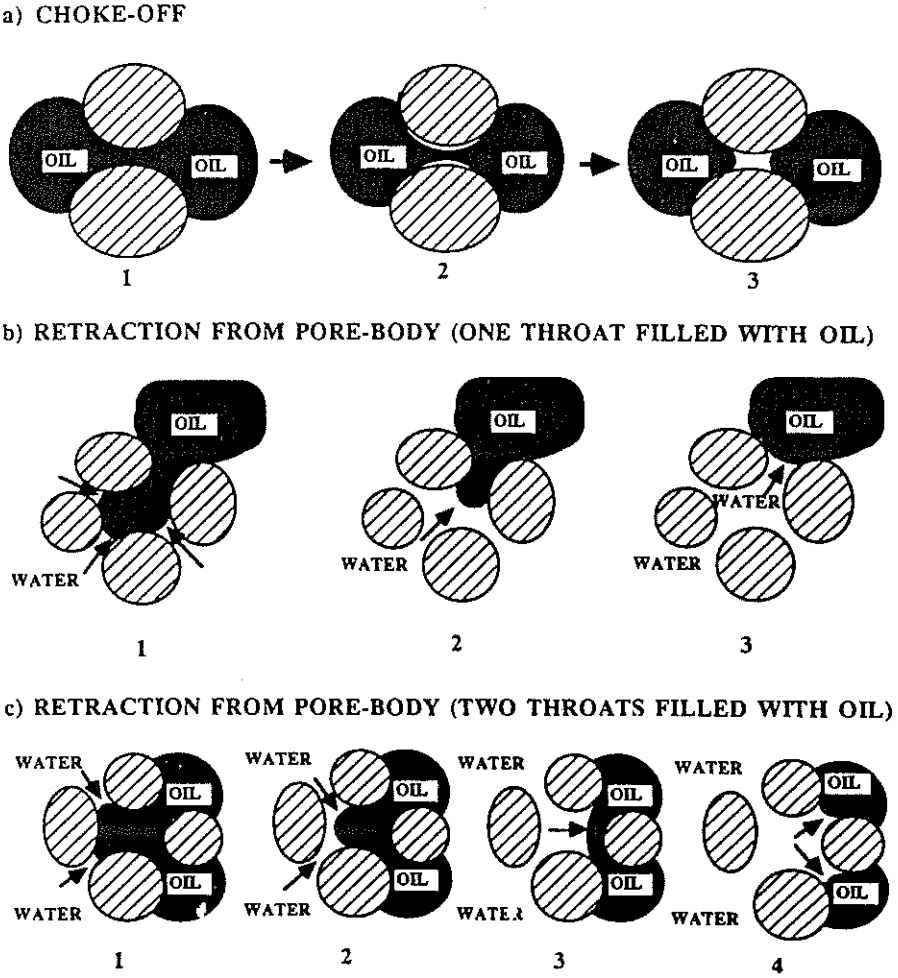

Fig. 5. Pore-level events in imbibition. *Choke-off* in pore-throat (a) or *retraction* of nonwetting phase from pore-body (b), (c). Capillary pressure at which each event takes place depends upon size of body or throat and configuration of interface (e.g. number of nearest neighbors containing nonwetting phase).

collapses if

$$P_c < 2H\sigma = \left(\frac{1}{R_1} - \frac{1}{R_2}\right)\sigma \approx \frac{\sigma}{r_t}$$

Here R_2 represents the radius of curvature in a direction roughly tangent to the centerline of the throat. For simplicity we have assumed that $2H = C/r_t$, where C is a constant of order unity which is estimated from the pore-structure and may be regarded as a parameter characterizing the porous medium (Li and Wardlaw, 1985). In the simulations presented below, $C = 1$ for consolidated medium, $C = 2/3$

for the medium of intermediate consolidation and $C = 0.6$ for the unconsolidated medium.

In *retraction* (Figure 5), as the capillary pressure is decreased the head meniscus within a pore-body retracts spontaneously through the adjoining pore-throats, ending in head menisci in adjoining pore-bodies. The capillary pressure at which retraction takes place in a given pore depends on the number of throats filled with nonwetting phase which are connected to that pore. If only one throat connected to the pore-body is filled with nonwetting phase, retraction takes place if

$$P_c < 2H\sigma \approx \frac{2\sigma}{r_b}.$$

This event defines r_b for that circumstance. If more than one adjoining pore-throat contains nonwetting phase, the interface can take-on configurations which have lower curvature and, hence, retraction will occur at smaller capillary pressures. The dependence of the capillary pressure necessary for retraction depends upon the geometry of the pores and interface within the pores (Lenormand and Zarcone, 1984; Li and Wardlaw, 1985). Because the geometry in a real system is quite complex, we have assumed that

$$2H = \frac{2}{r_b z_{nw}}$$

where z_{nw} is the number of adjoining pore-throats filled with nonwetting phase. Because curvature, $P_c/2\sigma$, controls most of the phenomena, we correlate our results below to this parameter rather than capillary pressure.

3.4. SATURATION DETERMINATION

Within our model, the saturation of the phases is calculated by summing the contributions of pore-throats and pore-bodies separately and assuming wetting phase coats the interior of the pore-space. Pore-bodies have the volume of a sphere of radius r_b. Pore-throats have the volume of cylinders of radius r_t and a length determined by subtracting the body radii at either end of the throat from the distance between pore-body centers. The saturation of wetting fluid in the nooks and crannies of the pore-space is determined from the irreducible wetting phase saturation, S_{wr}. Here we have assumed 0.18 for Berea (Salter and Mohanty, 1982), although we have recently come to believe that this number is somewhat too high, and 0.075 for sphere-pack (Dombrowski and Brownell, 1954). Micromodel studies indicate that, even excluding the nooks and crannies, the nonwetting fluid does not occupy whole pore-bodies. In addition, the partitioning of pore-space between pore-body and throat is somewhat arbitrary. For these reasons, we introduce a parameter x which is a measure of the relative contributions of the pore-throats and pore-bodies to the saturation. Hence, the saturation of nonwet-

ting fluid is

$$S_{nw} = (1 - S_{wr})[xS_t + (1 - x)S_b]$$

where S_t is the volume fraction of the pore-throats occupied by nonwetting phase and S_b is the volume fraction of pore-bodies occupied by nonwetting phase. The parameter, x, can be estimated by assuming that entire pore throats are occupied by nonwetting phase, in which case, x is the fraction of the pore-space taken up by pore-throats. Otherwise, x can be determined from the residual to the nonwetting phase for a flood started from irreducible wetting phase. In the simulations below, x was found to be 0.3 for the beadpack (consistent with entire pores being invaded by nonwetting phase as well as matching the largest residual) and 0.75 for sandstone (to match the largest residual).

3.5. RELATIVE PERMEABILITY CALCULATION

The permeability and average flow through each pore-throat or body is calculated by assigning conductances to the pore-throats and solving the system of equations generated by applying continuity at each pore-body. Koplik (1982) has laid out the methods of transcribing such a 'ball and stick' model of a porous medium into a network of hydraulic conductances. The hydraulic conductance associated with a pore-throat can be broken into three parts; an entrance contribution generated in going from pore-bodies to pore-throats, an exit contribution generated in going from throats back to pore-bodies, and a contribution for the pore-throat itself (Dagan *et al.*, 1982). The pore-throat itself can be envisioned as a capillary of radius, r_t, and length l bounded by fluid regions much wider than the capillary. The hydraulic conductance of the combination is then

$$g = \frac{r_t^3}{\left(3 + \frac{81}{\pi r_t}\right)}$$

where $q = (g/\mu)\,\Delta p$.

Here, q is the total fluid flow through a pore-throat and Δp is the pressure drop between the pore-bodies at the ends of the pore-throat. In single phase flow, we calculate the flux of fluid through the network by applying continuity at each pore-body and solving the resulting equations for the pressure at each pore-body using a computer. The permeability is calculated from its definition using the flux and the pressure drop across the network.

Relative permeability is calculated by regarding each phase as a separate sub-network of the network used in single phase flow and comparing the flux calculated through each sub-network to that in single-phase flow. The nonwetting phase sub-network consists of all the interconnected pore-bodies and pore-throats occupied with nonwetting phase. The wetting phase sub-network consists of all the pore-bodies and throats filled with wetting phase as well as nooks and crannies associ-

ated with the pore-bodies and throats occupied with nonwetting phase. As de scribed above, the pore-scale distribution of fluid in two-phase flow is calculatec by simulating the pseudo-static invasion of each phase as the applied capillary pressure changes. The fluid distribution calculation proceeds in increments of one pore-level event. At each step, a search is made over the entire interface to determine which pore-level event will occur with the smallest change in capillary pressure. After completing a number of steps, the fluid distribution and associated capillary pressure is saved. Relative permeability curves are generated assigning hydraulic conductances to the subnetworks associated with each phase and calculating fluid flux. Capillary forces are assumed to prevent flow normal to interfaces; hydrodynamic interactions between the phases are assumed negligible.

Despite the high level of contact between the wetting and nonwetting phases, there is little evidence that hydrodynamic interaction between the two phases is important. If hydrodynamic interaction between the two phases were important, it would manifest itself in the effect of viscosity ratio upon relative permeability and the effect of pressure gradients in one phase upon the flow rate of the other. A number of people have shown theoretically that if the nonwetting phase is much more viscous than the wetting phase there may be a lubrication effect in which the nonwetting phase relative permeability is larger at low wetting phase saturations than it would be for a unit viscosity ratio system (Yuster, 1951; Ehrlich and Crane, 1969; Larson, 1981; Danis and Jacquin, 1983; Levine and Cuthiell, 1986). However, when capillary forces dominate viscous forces, much of the evidence in the literature suggests that relative permeability is not affected appreciably by viscosity ratio or the direction of fluid motion (Dullien, 1979). A large number of researchers report no dependence of relative permeability on viscosity ratio (Muskat *et al.*, 1937; Leverett, 1938; Sandberg *et al.*, 1958; Osoba *et al.*, 1951; Donaldson *et al.*, 1966; Owens and Archer, 1971). In addition, Osoba *et al.* (1951) found that gas-oil relative permeability was the same in cocurrent and countercurrent flow and that the primary-drainage gas relative permeability was the same whether or not the liquid was flowing. Finally, some of the best evidence that phases do not interact very strongly are the experiments of Yadav *et al.* (1987). They showed that the relative permeability of both the wetting and nonwetting phases in drainage measured when the opposite phase was solidified *in situ* was the same as that typically measured for Berea.

Despite this evidence, it is clear that one cannot show that no situations exist in which interactions between the phases are important. In the work presented here, we have assumed that these hydrodynamic interactions are negligible. Thus, our model is limited to cases where this assumption is valid.

The hydraulic conductance of each throat is impacted by the fluids which occupy each of the three sections of that pore-throat. Each of the segments is either completely filled by wetting-phase, or primarily filled by nonwetting phase. The hydraulic conductance of a section filled with wetting phase is equal to that of single-phase flow. The nonwetting phase conductance of a throat-section primarily filled with nonwetting phase is assumed to be the same as single-phase flow,

consistent with the observation that low connate water saturations do not reduce the permeability to oil substantially. The hydraulic conductance of the wetting phase in a section primarily filled by nonwetting phase is reduced to a very small, but finite, value by the presence of nonwetting phase. We approximate the conductance of such a section by reducing its total hydraulic conductance by a factor equal to the square of the ratio of the area fraction taken up by wetting phase in thin films and nooks and crannies to the total area (i.e. flow rate is proportional to the square of the area available for flow). The total hydraulic conductance of each throat is then made up of the three contributions, and the total network conductance for each phase is calculated as before.

In the simulations presented below we have used networks of $20 \times 20 \times 20 = 8000$ pore-bodies with periodic boundary conditions applied in the two directions transverse to the flow direction. We believe that these are large enough to discern trends in capillary pressure and relative permeability. Because of the time and expense required however, we have not checked each set of curves to see if they would change with network size. Spot checks comparing results on cubic networks with $16 \times 16 \times 16$ and $32 \times 32 \times 32$ showed few differences. Results also changed little between different sets of random numbers, hence a single realization was used. The calculated relative permeability of a phase is least accurate when its saturation is low. Chatzis and Dullien (1982), Diaz *et al.* (1987), and Li *et al.* (1986) have discussed the effects of network size. They, respectively, report that networks of $18 \times 18 \times 12$, $15 \times 15 \times 15$, and $20 \times 20 \times 20$ pore-bodies are required to give satisfactory results. Wilkinson (1986) has discussed the impact of small network size upon relative permeability and capillary pressure in some detail. The major impact of using small networks is to increase the relative permeability of both phases and to shift the residual nonwetting phase to lower values.

The matrix of linear equations which must be solved to calculate the flow rate through the network is large, sparse and somewhat ill-conditioned. The periodic boundary conditions make the bandwidth very large. The nonwetting phase calculations were greatly facilitated by first stripping away the deadends and isolated structures before setting up the matrix solution. The matrix equations were solved using a preconditioned conjugate-residual method called the 'truncated Petrov–Galerkin–Krylov method' with modified incomplete LU factorization as a preconditioner (available in the Yale iterative sparse matrix package, Elman *et al.*, 1983; Schultz *et al.*, 1983). Constant-pressure boundary conditions were applied along the inlet and outlet faces. Roughly two-thirds of the computation time was spent solving for the relative permeability, most of the remainder was spent doing the searches involved in the pseudo-static invasions.

4. Results

Results are presented here which demonstrate the impact of various pore-morphological descriptors on capillary pressure and relative permeability. Although results have been generated for both regular and random lattices of different coordination

numbers, only results for the regular, cubic lattice will be shown. As stated above, the impact of coordination number and lattice randomness has been found to be secondary. The impact of three major descriptors will be emphasized: aspect ratio, pore correlation, and pore-size distribution.

All pore-level model results presented are typified by Figure 6. Results, capillary pressure and relative permeability, are presented for primary drainage, imbibition,

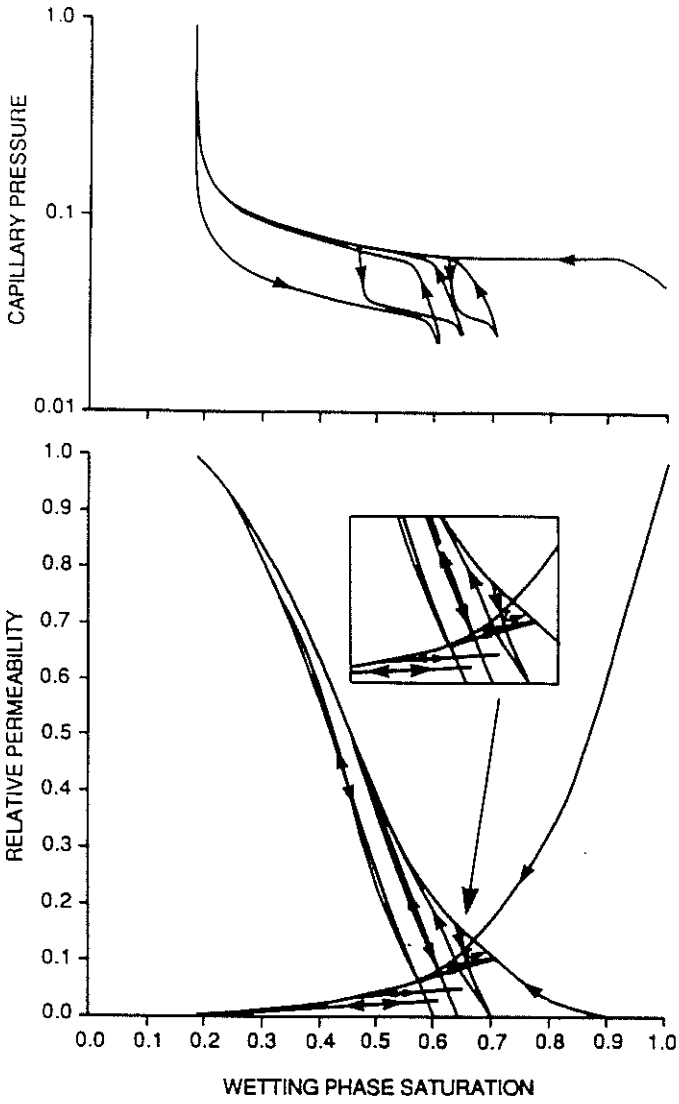

Fig. 6. Pore-level model predictions of hysteresis in relative permeability and capillary pressure for high-aspect-ratio porous medium, typical of consolidated sandstone, e.g. Berea sandstone.

and secondary drainage. Typically, three scanning loops are shown, where the primary drainage cycle is stopped at different nonwetting phase saturations. Since the permeability to nonwetting phase at irreducible wetting phase saturation is assumed to equal the total medium permeability, normalization of the relative permeabilities by either extreme is equivalent. In order to keep the capillary pressure curves on the same scale we have plotted the curvature, $P_c/2\sigma$, in units of μm^{-1}.

The results to be presented may be understood within a general context. Relative permeability and capillary pressure are determined by the geometric structure of the phases. For the nonwetting phase, continuous flowing pathways must exist which span the network in order to generate permeability. The number and effectiveness of these pathways determines its magnitude. The wetting phase always spans the network (is continuous). The magnitude of the wetting phase relative permeability is determined by the number of segments along the various flowpaths which are filled primarily by nonwetting phase. The geometric structure is, in turn, determined by the pore structure (through its impact on the different pore-level events) and the saturation history. The relative importance of choke-off and retraction during imbibition is shown to be a major factor causing the differences in the geometric structure of the phases which result in hysteresis.

4.1. SINGLE PHASE PERMEABILITY

The single phase permeability predicted using this network model agrees within an order of magnitude with that of actual porous media. Simulated permeabilities are usually larger. The single phase permeability of random Voronoi networks was found to be roughly 20% lower than that of regular networks (for $z = 6, 8$), hence the random topology and increased variance of conductance distribution lead to a small change in absolute permeability but no substantial change in relative permeability.

4.2. EFFECT OF ASPECT RATIO ON HYSTERESIS

The single most important feature determining the pattern of hysteresis is the pore-body to pore-throat aspect ratio. Other features of the pore-structure must be changed, however, to reproduce all the details of relative permeability of a particular porous medium; we describe these other effects in the following sections. Aspect ratio is important because it determines the relative importance of the choke-off and retraction mechanisms. In *high aspect ratio media*, those in which pore-bodies are much larger than pore-throats, the choke-off mechanism predominates the retraction mechanism.

Berea sandstone is an example of a medium with a *high aspect ratio*. Figure 6 shows pore-level modeling results based on the 'sandstone' pore-size distribution described above. The hysteresis behavior is typical of that exhibited by consoli-

dated media. The primary drainage relative permeability to the nonwetting phase is greater than that of imbibition which, in turn, is the same as secondary drainage (c.f. Figure 1). Less hysteresis occurs in the wetting phase; primary drainage is slightly greater than imbibition which in turn is the same as secondary drainage. We have measured steady-state relative permeability of strongly-wetting fluids in Berea sandstone and hysteresis behavior (particularly wetting phase) which is qualitatively similar to that predicted by the model (Figure 7). Scanning loops in nonwetting phase relative permeability predicted by the pore-level model resemble those measured by Geffen *et al.* (1951). The absence of hysteresis between imbibition and secondary drainage occurs because the invasion of nonwetting phase in drainage, and choke-off in imbibition, both depend only upon throat size. Hence, the nonwetting phase occupies the same pore-throats in both cycles, resulting in approximately the same relative permeability. The nonwetting phase relative permeability in primary drainage is greater than that in secondary drainage because nonwetting phase becomes disconnected during imbibition, hence a larger fraction of the nonwetting phase is active in transport during primary drainage. The wetting phase relative permeability in primary drainage is greater than that in secondary drainage because disconnected nonwetting phase interrupts the channels filled with wetting phase more effectively than connected nonwetting phase. This distribution of the nonwetting phase is corroborated through analysis of its geometric structure.

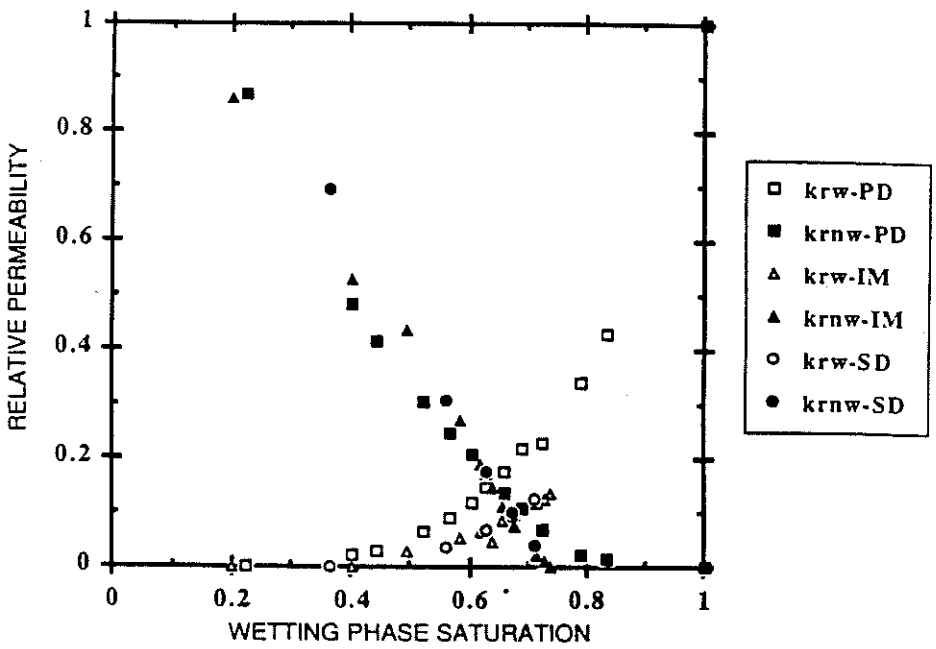

Fig. 7. Steady-state measurements of relative permeability of strongly wetting fluids in fired and acidized Berea sandstone.

The geometric structure of a phase within a porous medium can be described in terms of its flowing, dendritic and isolated fractions. The *flowing fraction* (also called the backbone, or effective fraction) is the fraction of the saturation contained in regions which are connected to both the inlet and outlet by at least one nonintersecting path, and consequently contains flowing fluid. The *dendritic fraction* of a phase is connected to the flowing fraction of that phase but does not exhibit flow itself. The fluid in these pores can be recovered in a miscible displacement within a phase by diffusion into the flowing fraction. The flowing and dendritic fractions together constitute the recoverable fraction; the remainder is *isolated*. The *isolated fraction* of a phase is completely surrounded by the other phase, through which no diffusion is assumed to occur. This material is therefore not recoverable. All fluid particles contained within the flowing fraction must be accessible to the medium surface by at least two independent paths, one to the outlet and one to the inlet, over which a pressure drop must occur. The fluid particles contained in the dendritic fraction must be connected to the surface by continuous pathways filled by the fluid in question, but some portion of this pathway must be redundant, thereby eliminating the possibility that a pressure drop can exist within this fraction.

The relative permeability of the nonwetting phase can be understood in terms of the geometric structure of that phase. The saturation dependence of the dendritic, flowing and isolated fractions of the nonwetting phase predicted by the pore-level model (Figure 8) are in qualitative agreement with those measured by Salter and

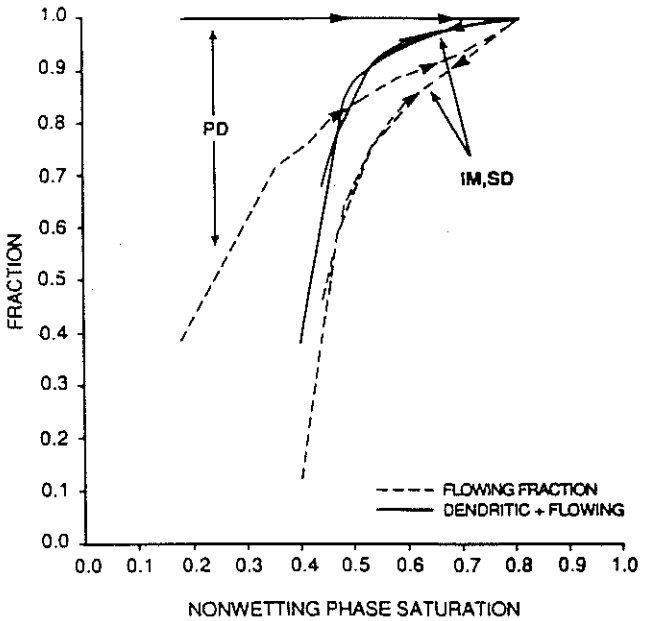

Fig. 8. Flowing and dendritic fractions of nonwetting phase for consolidated porous medium predicted by pore-level model are in qualitative agreement with those of Salter and Mohanty (1982).

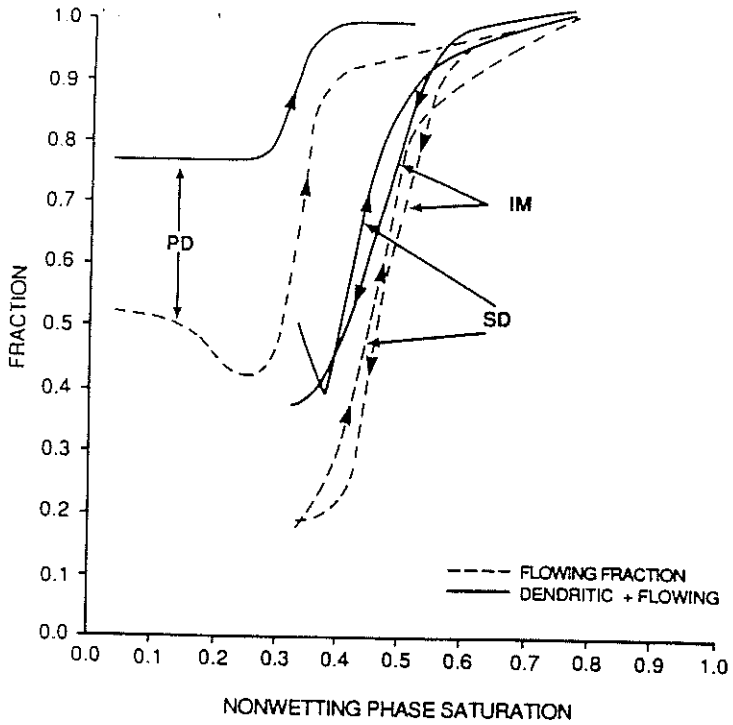

Fig. 9. Flowing and dendritic fractions of nonwetting phase measured for fired and acidized Berea sandstone after Salter and Mohanty (1982).

Mohanty (1982, Figure 9). All the phase fractions in secondary drainage are essentially the same as in imbibition. In primary drainage, however, little or no isolated fraction and a somewhat larger dendritic fraction exist at low saturation. These differences between primary drainage and the later cycles can be understood in terms of the relative importance of choke-off in the various cycles. Since capillary pressure is always increasing in primary drainage, choke-off plays a very minor role. Thus, few isolates are created. During imbibition, however, choke-off is very important (n.b., at residual, all of the nonwetting phase is isolated). During secondary drainage, much of this nonwetting phase remains isolated until the saturation becomes fairly high. Thus, the differences between the phase fractions in the cycles are greatest at low saturation. There is a minor difference between the predictions of the pore-level model and experimental data reported by Salter and Mohanty (1982). At low saturations, the dendritic and flowing fractions found experimentally become independent of saturation whereas they decrease in the pore-level model. We have not fully understood why this difference exists but note that, in this region, sample size effects will cause the pore-level model to be less accurate and that flow in this regime may include a mixture of drainage and imbibition mechanisms independent of the process.

Figure 10 shows the saturation in the backbone and dendritic fractions plotted

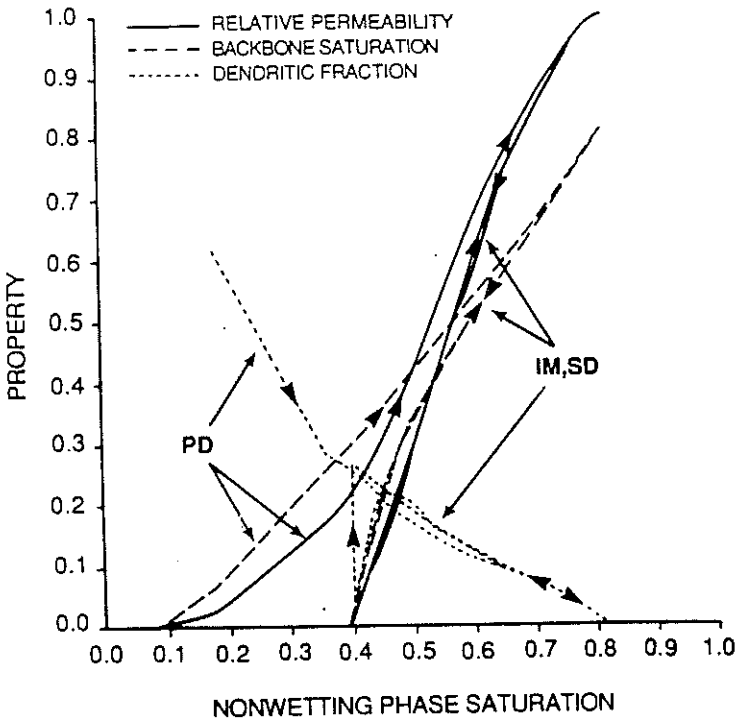

Fig. 10. Relative permeability, backbone saturation and dendritic fraction of nonwetting phase for high-aspect-ratio porous medium predicted by pore-level model. The hysteresis pattern in backbone fraction and relative permeability are the same.

along with the relative permeability of the nonwetting phase. The dendritic fraction is larger in primary drainage at low saturations and nearly the same as in imbibition and secondary drainage at high saturations. Because relative permeability and backbone saturation have the same general form, it is apparent that the backbone structure of the nonwetting phase, and not the size of the pores it occupies, is the major determinant of the relative permeability to the nonwetting phase. Clearly, stagnant saturation (the sum of the isolated and dendritic fractions) cannot contribute to permeability. Thus, the sum of the isolated and dendritic saturations can be viewed either as increasing the saturation required to yield a given permeability, or decreasing the permeability which occurs at a given saturation. If relative permeability is plotted vs. backbone saturation, as it is in Figure 11, hysteresis disappears. This observation is similar to those of Goddard *et al.* (1962) who explained, based on experiments that "electrical conductivity and diffusivity depend upon the total volume of conducting phase and the nature of its interconnections but are not affected directly by the pore-size distribution" and who found that electrical conductance curves have the same hysteresis behavior as relative permeability. Salter and Mohanty (1982) also found experimentally (see Figure 12) and through pore-level modeling (Mohanty and Salter, 1982) that the relative

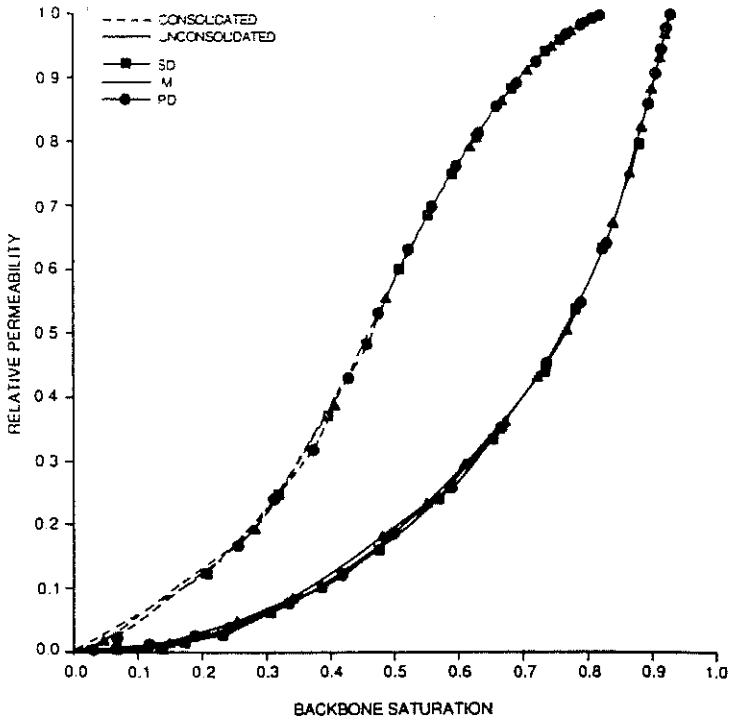

Fig. 11. Pore-level model predictions of the dependence of relative permeability of the nonwetting phase upon saturation of nonwetting phase in the backbone fraction for high- (consolidated) and low- (unconsolidated) aspect ratio media. The lack of hysteresis shows that relative permeability depends primarily upon the saturation in the backbone fraction.

permeability depends primarily on the backbone saturation. This observation is consistent with the conceptual picture provided by percolation theory (Kirkpatrick, 1972; Larson *et al.*, 1981; Heiba *et al.*, 1982; Wilkinson, 1986; Katz and Thompson, 1987) that a large part of relative permeability behavior can be understood as near-critical behavior, in which the long range structure is important but the particular sizes of pores and values of hydraulic conductances are not. These same ideas hold for systems with low aspect ratios but details in the geometrical structure of the phases change. The changes that do occur are examined briefly below.

A pack of monodisperse beads is an example of a *low-aspect-ratio medium*. Figure 13 shows pore-level modeling results for the 'beadpack' pore-size distribution described above. The hysteresis behavior is typical of that exhibited by unconsolidated media (e.g. Naar *et al.*, 1962). The imbibition relative permeability to the nonwetting phase is greater than that in primary drainage which is similar to secondary drainage. Almost no hysteresis is present in the wetting phase. The residual nonwetting phase is significantly smaller than that in consolidated media. The nonwetting phase relative permeability in imbibition is greater than that in drainage because there is little dendritic fraction. Hence, for a given saturation,

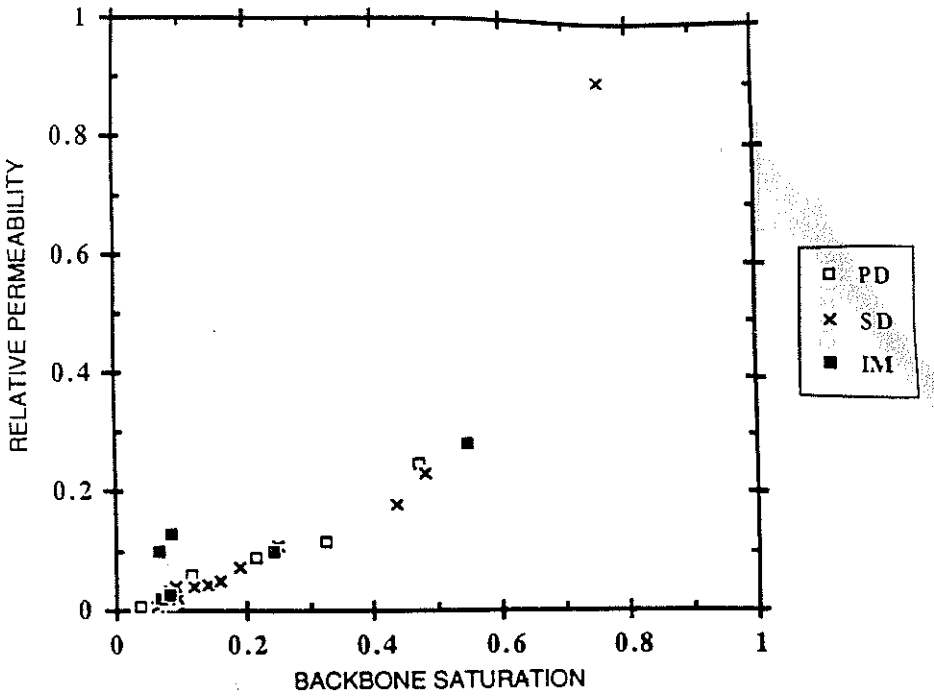

Fig. 12. Dependence of relative permeability of the nonwetting phase upon saturation of nonwetting phase in the backbone fraction for Berea sandstone. Data are taken from work of Salter and Mohanty (1982).

more nonwetting phase is active in transport. The wetting phase relative permeability in primary drainage is only slightly larger than that in secondary drainage because very little nonwetting phase is trapped during imbibition. Scanning loops predicted by the pore-level model are shown in Figure 13. These loops have regions where the imbibition nonwetting phase relative permeability is nearly horizontal and should probably be regarded as an extreme limiting case or an idealization resulting from the crude approximations used for the retraction criteria. We have seen no data in the literature which support or refute this result. Dominance of the retraction mechanism in low aspect ratio media leads to the differences in behavior compared with media with high aspect ratio. Retraction tends to occur at the lowest coordinated pore-bodies first preventing the formation of dendritic structure in the nonwetting phase. Pore-level model predictions of the dendritic and backbone saturations and relative permeability of the nonwetting phase (Figure 14) support this view of the hysteresis behavior and show that the backbone saturations and relative permeability have similar hysteresis behavior. Although we have made no attempt to find the magnitude of the effect, the reduction in the amount of nonwetting phase dendritic fraction which exists during imbibition compared to that in primary drainage at the same overall saturation, should result in less capacitance within the nonwetting phase (asymmetry in tracer

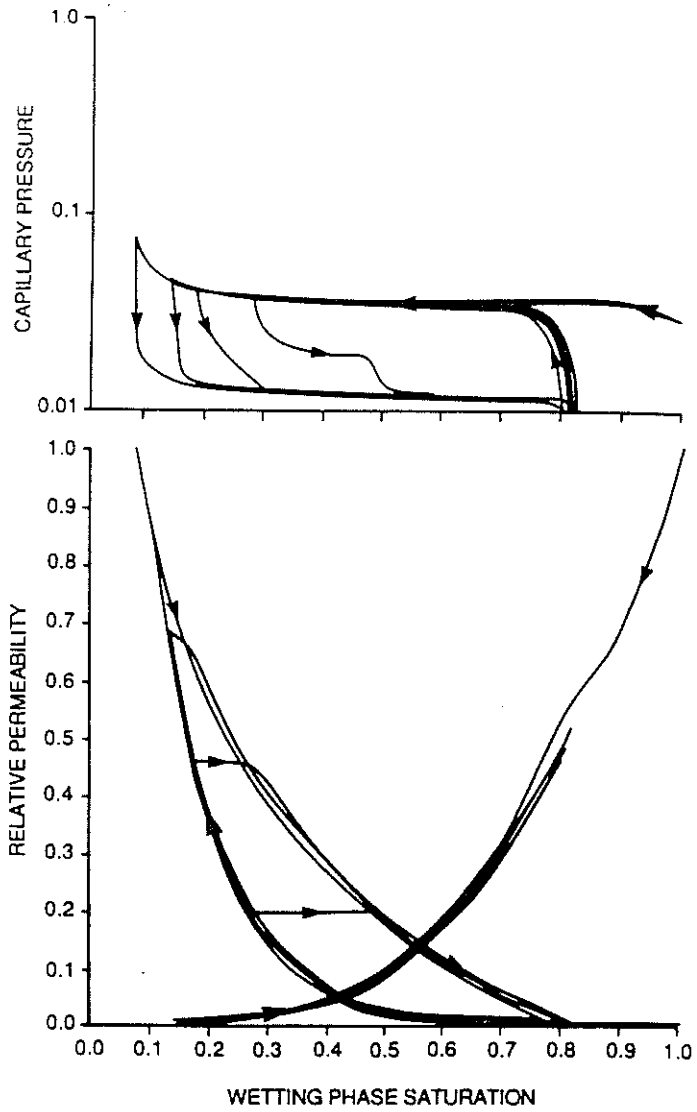

Fig. 13. Pore-level model predictions of hysteresis in relative permeability and capillary pressure for low-aspect-ratio porous medium, typical of sand or bead pack.

concentration profiles due to mass transfer with stagnant regions), during a miscible displacement in imbibition. It is also worth noting that the pattern of hysteresis predicted for unconsolidated media is of the same general form as that used by Gladfelter and Gupta (1978) in their explanation of 'humps' in saturation profiles, although the origin of the hysteresis in the relative permeability they measured is probably different.

Pore-level predictions of the hysteresis behavior of a medium of *intermediate*

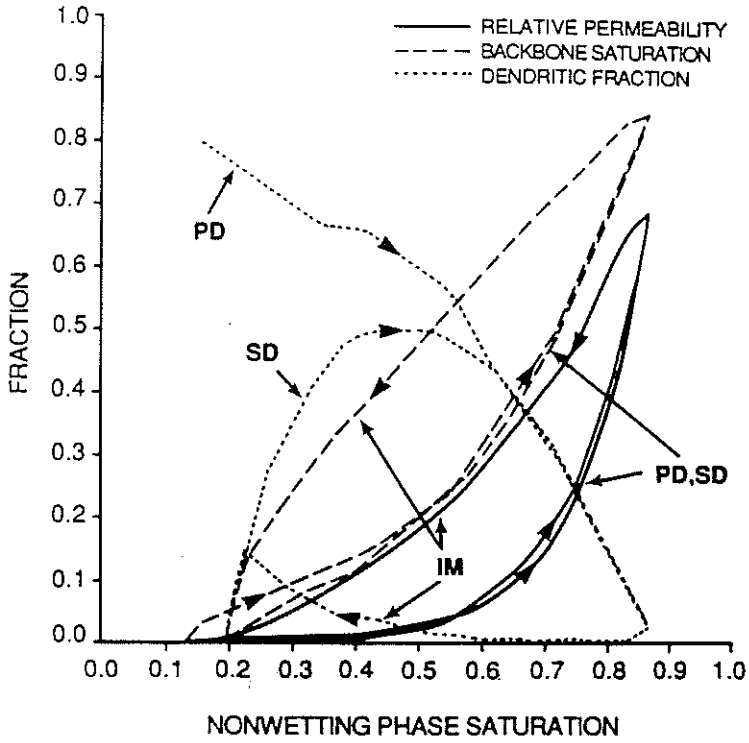

Fig. 14. Pore-level model predictions of relative permeability, backbone saturation and dendritic fraction of nonwetting phase for low-aspect-ratio porous medium. Low aspect ratio media have few deadends in imbibition because of the retraction mechanism. Relative permeability and backbone saturation have the same hysteresis pattern.

aspect ratio are shown in Figure 15. These simulations were generated by keeping the pore-body and pore-throat distributions for a consolidated medium (sandstone) and changing the constant C from 1 to 2/3. Essentially no hysteresis is observed for the wetting phase. For the nonwetting phase, these predictions have the same general form observed by Colonna *et al.* (1972). Primary drainage relative permeability is smaller than imbibition relative permeability; secondary drainage relative permeability is less than that in primary drainage. Scanning loop behavior is very complex, with a small region in which imbibition relative permeability is independent of saturation followed by a region where relative permeability decreases with saturation (Figure 1). Unlike consolidated and unconsolidated media, where relative permeabilities measured during scanning loops stay within 'bounding curves' (generated from an experiment run to irreducible wetting phase saturation, back to residual and back to irreducible again), successive scanning loops for intermediate aspect ratio media cross each other. Figure 16 shows the dendritic fraction, backbone saturation and relative permeability within an intermediate hysteresis loop. The nonwetting phase relative permeability and backbone saturation have the same hysteresis behavior, as observed for the media with more

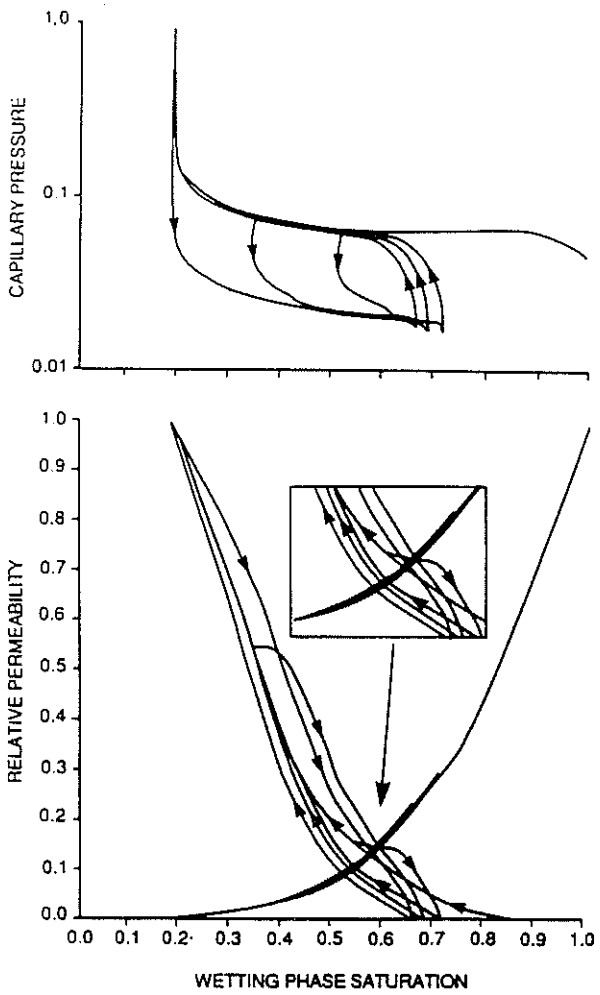

Fig. 15. Pore-level model predictions of hysteresis in relative permeability and capillary pressure for porous medium with intermediate aspect ratio; similar curves have been measured by Colonna *et al.* (1972).

extreme aspect ratios discussed previously. This result gives strong evidence that once the fluid distribution is determined, the relative permeability is set. The aspect ratio controls the mechanisms which generate the fluid distributions. The dependence of the dendritic and backbone fractions upon saturation during imbibition shows that the flat region in the relative permeability curve results from the retraction process consuming the dendritic fraction; the region of decreasing relative permeability corresponds to choke-off consuming the backbone, thereby increasing the dendritic fraction.

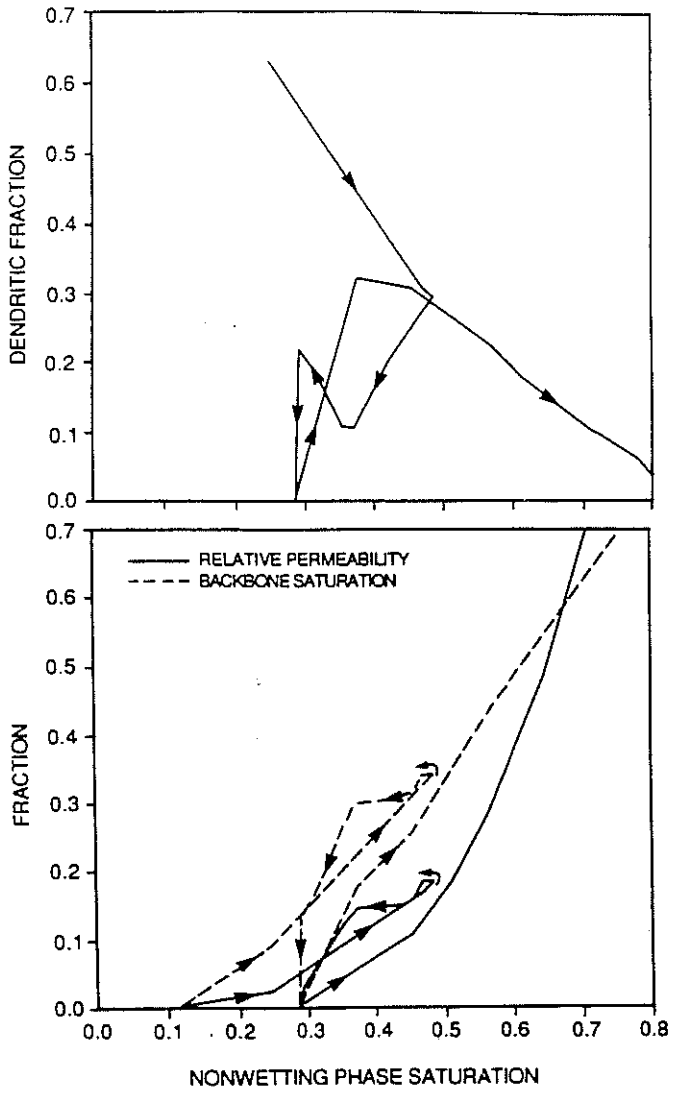

Fig. 16. Pore-level model predictions of relative permeability, backbone saturation and dendritic fraction of nonwetting phase for intermediate-aspect-ratio porous medium for an intermediate hysteresis loop.

4.3. EFFECTS OF CORRELATION IN PORE-STRUCTURE

Correlation in pore structure can be divided into at least two types: correlation between the sizes of pore-bodies and their neighboring pore-throats (throat-body correlation), and correlation between neighboring pore-throats (throat-throat correlation) or neighboring pore-bodies (body-body correlation). Correlations of these types can be formulated in a variety of different ways. Different types of correlations may also be mixed. We have attempted to determine the impacts such

correlations have on relative permeability and capillary pressure, rather than to determine their cause or measure their magnitude. It is difficult to implement correlation without impacting some other part of the pore morphological description. For example, if throat-body correlation is implemented (while keeping the pore-body and -throat size distributions constant), changes in aspect ratio generally occur. Thus, it is difficult to determine which input is causing the observed change in the transport coefficient of interest. We have not attempted to make an exhaustive study of different formulas for correlation. Thus, it is somewhat difficult to make all-encompassing generalizations. We present here, instead, what appear to be general findings, at least for the types of correlation we have studied.

The simplest case independently assigns pore-throats and pore-bodies from their respective distributions by using a random number generator to assign numbers (from a uniform distribution) to each pore-body or pore-throat. To assign a radius to each pore-throat (pore-body), we find the radius such that the cumulative probability is equal to the random number assigned to that throat (body), i.e. if Ω is the random number, we find r such that $\Omega = \int_0^r d\rho f(\rho)$, where $f(\rho)$ is the probability density function. In building-in correlation, we have assigned these random numbers to throats (Ω_t) and bodies (Ω_b) using several different schemes. To normalize so that the distribution of pore-sizes does not change from scheme to scheme, we order the random numbers and reassign them so that they form a uniformly distributed set, i.e. set $\Omega_{ji} = i/(n+1)$ where n is the number of random numbers (number of bodies or throats) and i refers to the position in the ordering ($j = b$ or t). This normalization is similar to that used by Li *et al.* (1986).

We have generated correlation in a number of different ways to verify that the results are not highly dependent upon the details of the generation scheme, only the extent of correlation. Spatial correlation was generated by first assigning random numbers to each pore-body. Next numbers, Ω_t, were assigned to each pore-throat using the random numbers assigned to the pore-bodies at each end of the pore-throat, Ω_{b1} and Ω_{b2}, according to the following prescriptions,

(1) base case, $\Omega_t = \omega$ a random uniformly distributed number,
(2) $\Omega_t = \Omega_{b1}$ or $\Omega_t = \Omega_{b2}$ with equal probability,
(3) $\Omega_t = \omega\Omega_{b1} + (1-\omega)\Omega_{b2}$,
(4) $\Omega_t = (\Omega_{b1}\Omega_{b2})$,
(5) $\Omega_t = ((\Omega_{b1}\Omega_{b2})^{1/2} + 1. - ((1-\Omega_{b1})(1-\Omega_{b2}))^{1/2})/2$,
(6) $\Omega_t = (\Omega_{b1} + \Omega_{b2})/2$.

These are in order of increasing degree of correlation as judged from variograms measured for samples which are periodic in all (three) directions (Figure 17). The variogram shows that the range of influence of these schemes is, as one might expect from the prescription, only to nearest neighbors. The above correlations were used on both Voronoi and cubic networks with similar results. Another type of correlation was developed only on the cubic network by thinking of the network as a 3D checkerboard and assigning

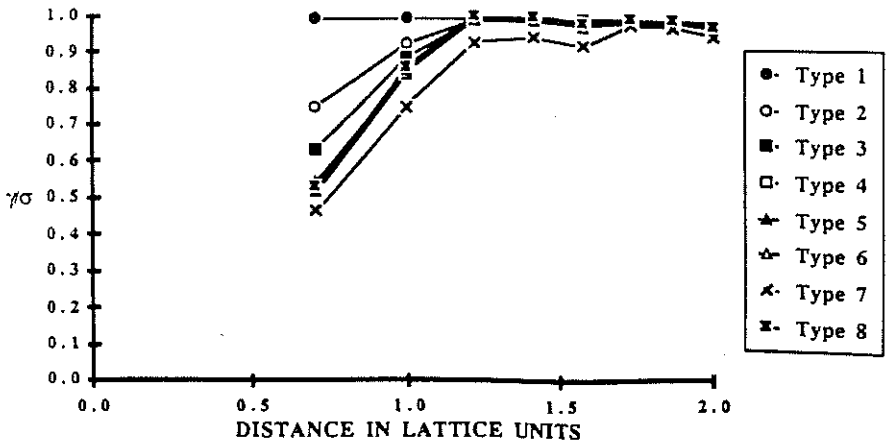

Fig. 17. Variograms of pore-throat radii for different correlation schemes on cubic networks. $\gamma(r_j)$ is the average of $(r_t(x_i) - r_t(x_i + r_j))^2/2$ over all the centers of throats, x_i, for a cubic network of $20 \times 20 \times 20$ pore-bodies. σ is the variance of the pore-throat radius distribution. The data points correspond to the different distances between pore-throats, the smallest is the lattice spacing divided by $\sqrt{2}$, there are two types of neighbors one lattice unit away (one type of neighbor which shares a common pore-body, the other type whose centerline is parallel to the reference throat) and so forth. Correlation between pore-throats is only significant in nearest neighbors which share a pore-body except type 7 which has slightly more extensive correlation and type 1 which has none.

(7) Ω_b(red) = Ω_b(black) neighbor with equal probability and $\Omega_t = (\Omega_{b1} + \Omega_{b2})/2$

This scheme creates a larger degree of correlation than 1) through 6).

We have deduced from simulations that the effect of correlation upon absolute permeability is to increase the permeability. For example, using the consolidated medium pore-size distribution, the increase in absolute permeability ranged from between 10 and 60% depending upon the degree of correlation. The largest increase occurred when pore-bodies and pore-throats were correlated. The increase in permeability was partially due to an increase in the average conductance associated with pore-throats but cannot be attributed to this alone; the permeability divided by the average conductance increased by between 10–40%. These observations are consistent with those of Katz and Thompson (1987) who have demonstrated that the majority of the hydraulic conductance of a medium is contributed by relatively few paths of high hydraulic conductance; correlation has the effect of increasing the probability and/or hydraulic conductance of such paths.

In *high-aspect-ratio media*, spatial correlation among throats tends to decrease the breakthrough and residual nonwetting phase saturations, as well as to decrease the curvature of the relative permeability curves during primary drainage and increase it in secondary drainage (Figure 18). Moreover, throat-throat correlation generally increases the nonwetting phase relative permeability and drops the wetting phase relative permeability slightly. The effect of correlation upon waterflood behavior is to increase the oil recovery at water breakthrough. The wetting phase

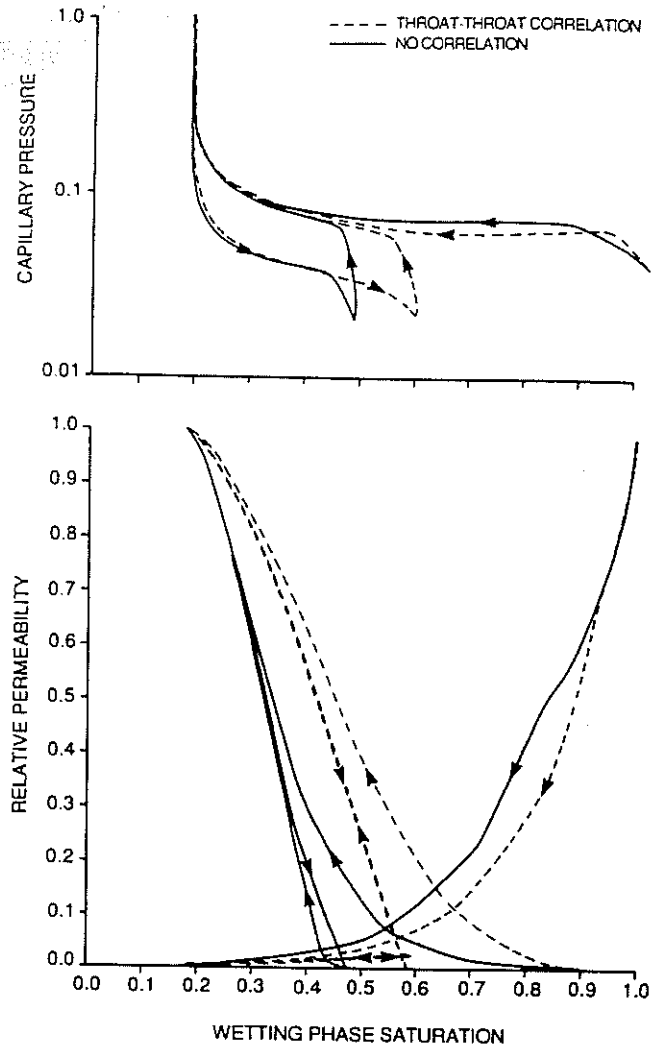

Fig. 18. Effect of throat-throat correlation (type 6) upon relative permeability and capillary pressure for high-aspect-ratio medium. Relative permeability of the nonwetting phase increases and relative permeability of wetting phase decreases with increasing amount of correlation.

saturation at which the two relative permeabilities are equal is higher and relative permeability there is larger. These observations are consistent with the results of Kirkpatrick (1973) who found that the effective conductivity (analogous to relative permeability) was higher in correlated systems and the percolation threshold (analogous to residual) was lower.

Some evidence, although circumstantial, indicates that correlation between pore-throats may occur to a greater degree in consolidated media than in unconso-

lidated media. Inasmuch as the pore-throats control fluid flow, the magnitude of the dispersivity during single phase flow measures the correlation in pore-structure (Hulin *et al.*, 1986). The ratio of the dispersivity to the grain size in consolidated media is roughly an order of magnitude higher in consolidated media (of the order of 10 for Berea sandstone, Salter and Mohanty 1982) than in unconsolidated media (of the order of 1, Hulin *et al.*, 1986). The relative permeability predictions of our pore-level model better approximate the behavior of consolidated media when correlation is included. These considerations led us to use type 6 correlation in the results presented for consolidated media in the previous section; no correlation between throats or bodies was used for the unconsolidated media predictions.

In our 'checkerboard' model, each pore-throat connects one black and one red pore-body. Another type of throat-throat correlation is generated by assigning to all the pore-throats the random number associated with their neighboring black pore-body.

(8) $\Omega_t = \Omega_b(\text{black})$

This step has the effect of keeping some pore-bodies unoccupied by nonwetting phase even at high nonwetting phase saturations (in primary drainage) and accentuates the dependence of the residual nonwetting phase saturation on the maximum nonwetting phase saturation previously achieved, even at high nonwetting phase saturations (Figure 19). This type of nonwetting phase relative permeability hysteresis pattern has been observed by Heaviside *et al.* (1983) in alumina.

We find only minor effects due to throat-body correlation. These effects were tested by comparing cases in which we assigned new random numbers, Ω_b, after choosing Ω_t with cases in which the set of Ω_b used to generate Ω_t was used to generate pore-body radii. Such correlation shifts $k_{rnw}{}^{IM}$ and $k_{rnw}{}^{SD}$ up and to the right, towards $k_{rnw}{}^{PD}$ (Figure 20). Thus, throat-body correlation leads to less hysteresis.

In *media of low aspect ratio*, correlation has the same impact on primary drainage and imbibition relative permeabilities as in high aspect ratio media (Figure 21). Correlation between neighboring pore-throats increases the nonwetting phase and slightly decreases the wetting phase relative permeabilities, while decreasing the difference between imbibition and drainage relative permeability. Throat-body correlation has little effect upon relative permeability. Some types of correlation lead to hysteresis behavior which is different than that described above. One example is type 4 correlation in which the wetting phase relative permeability is slightly higher in imbibition than in drainage (Figure 22). The checkerboard-type correlation also leads to somewhat more complex behavior (Figure 23). Nonwetting phase relative permeability is greater in imbibition than in primary drainage for hysteresis loops which reach moderate nonwetting phase saturations, while imbibition is less than primary drainage when the hysteresis loops cycle back at low saturations (secondary drainage relative permeability is always below primary drainage). In addition, more trapping occurs at low nonwetting phase saturations

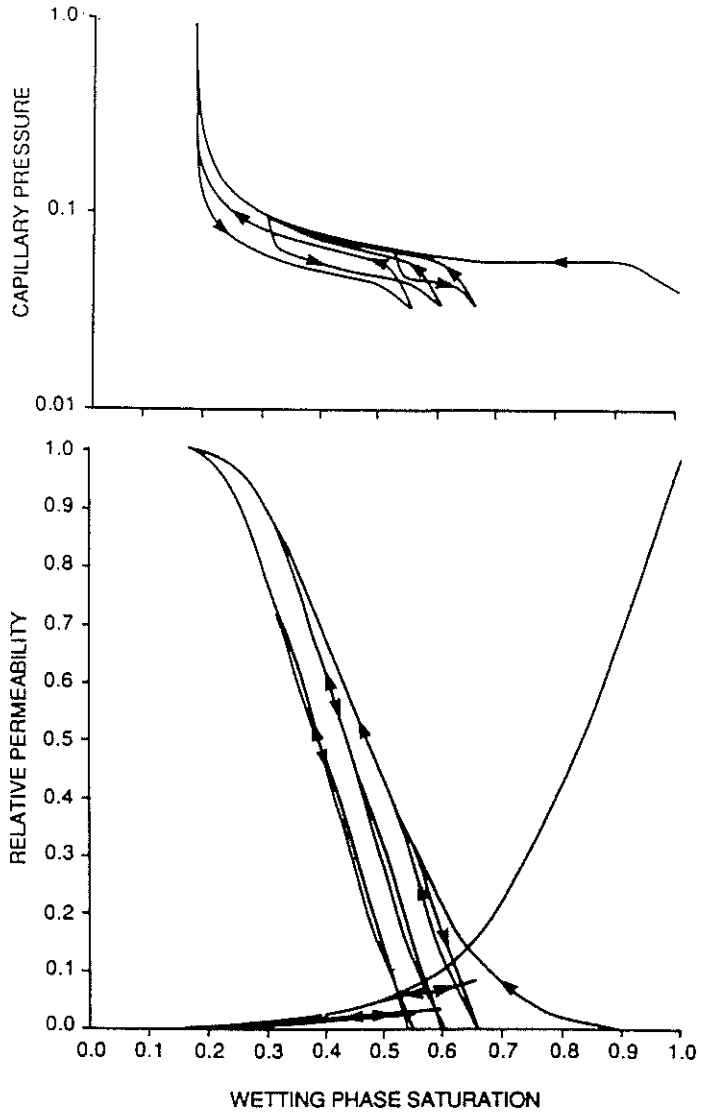

Fig. 19. Pore-level model predictions of hysteresis in relative permeability and capillary pressure for high-aspect-ratio medium with type 8 correlation, i.e. throats around 'black' pore-bodies of 3D checker board have the same size (bodies and throats are not correlated).

when this type of correlation is present. Hence, correlation in pore-structure can lead to a variety of hysteresis behaviors.

4.4. EFFECT OF PORE-SIZE DISTRIBUTION

In general, small changes in pore-size distribution do not change the resulting relative permeability predictions significantly. To demonstrate the effect of pore-

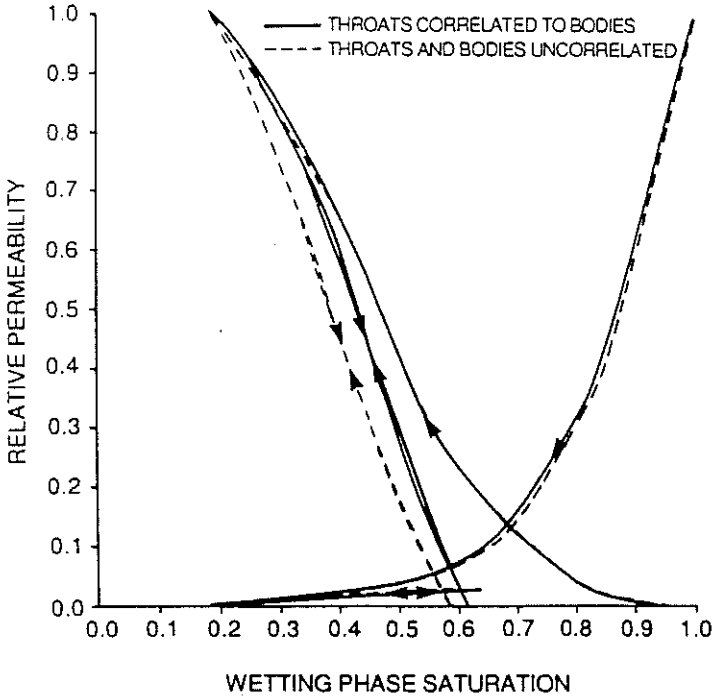

Fig. 20. Pore-level model predictions of the effect of throat-body correlation upon hysteresis in relative permeability for high-aspect-ratio medium with type 7 correlation. Nonwetting phase relative permeability in imbibition is higher when throats and bodies are correlated.

size distribution, we have run a limited number of cases in which the width of the pore-throat and/or pore-body size distributions was narrowed to one micron. A comparison of relative permeability and capillary pressure predictions for a consolidated media (Type 6 correlation with bodies and throats correlated and the pore-size distribution given in Figure 4), with those for a similar medium but a narrow pore-throat size distribution appears in Figure 24. As expected, the capillary pressure curve is much flatter with the narrow pore-size distribution. The wetting phase relative permeability is similar for both cases while differences occur in the nonwetting phase relative permeability. Whereas k_{rnwPD} for the narrow pore-size distribution medium is convex upward over the whole saturation, becoming linear only at high nonwetting phase saturations, the base case has an s-shape. The convex upward shape is due to overall connectivity or percolation effects; these are more apparent in primary drainage because of the higher dendritic fraction. The pore-size distribution creates the s-shape because the progressively smaller pore-throats contribute disproportionately less to the permeability ($g \sim r_t^3$) than to saturation ($S_t \sim r_t^2$). The failure of effective medium theory of relative permeability, as proposed by Levine and Cuthiell (1986), to show the concave upward behavior can be understood in terms of near-critical percolation behavior.

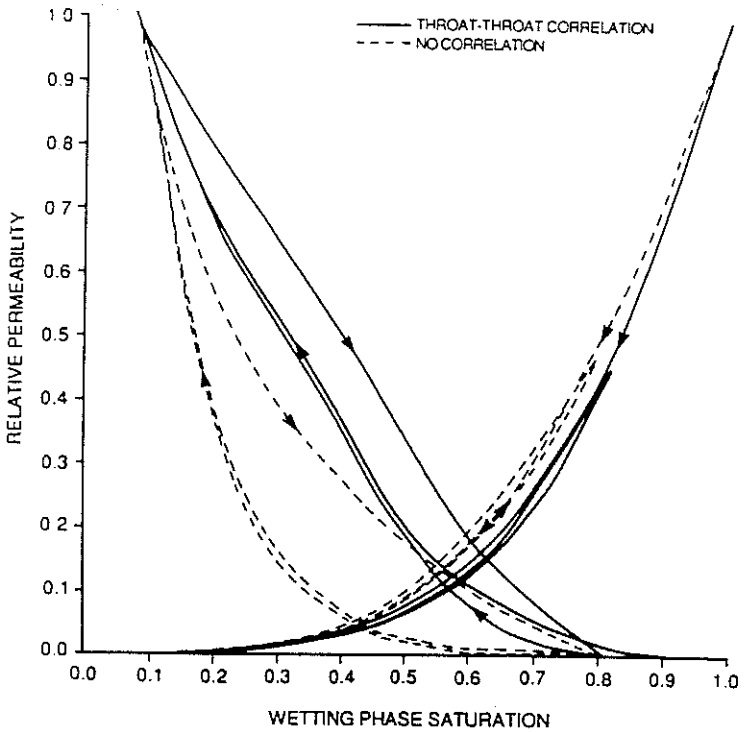

Fig. 21. Effect of throat-throat correlation (type 6) upon relative permeability for low-aspect-ratio medium. Relative permeability of the nonwetting phase increases and relative permeability of wetting phase decreases with increasing amount of correlation.

Effective medium theory does not include any provision for the long-range structure and, hence, leads to linear dependence of relative permeability upon saturation. However, the effect of nonwetting phase entering progressively smaller pores (at high nonwetting phase saturations) is modelled well by effective medium theory.

To evaluate the effect of correlation in pore structure on these conclusions we conducted studies with no correlation. Figure 25 shows relative permeability predictions for three cases with no correlation: one with the pore-size distribution for consolidated medium and one each with narrow pore-throat and pore-body size distributions (with the same average value). As one might expect, because the permeability is primarily controlled by the throat-size (as is the distribution of fluids on the pore-scale in a high aspect ratio medium), changing throat-size distribution has a larger effect on relative permeability. In fact, a case with a narrow pore-throat size distribution and a case with both narrow throat and body size distributions are nearly identical (for this reason the latter is not shown). As was the case in Figure 24, the predictions with a narrow throat-size distribution show a concave-upward rather than s-shape k_{rnwPD} The wetting phase relative

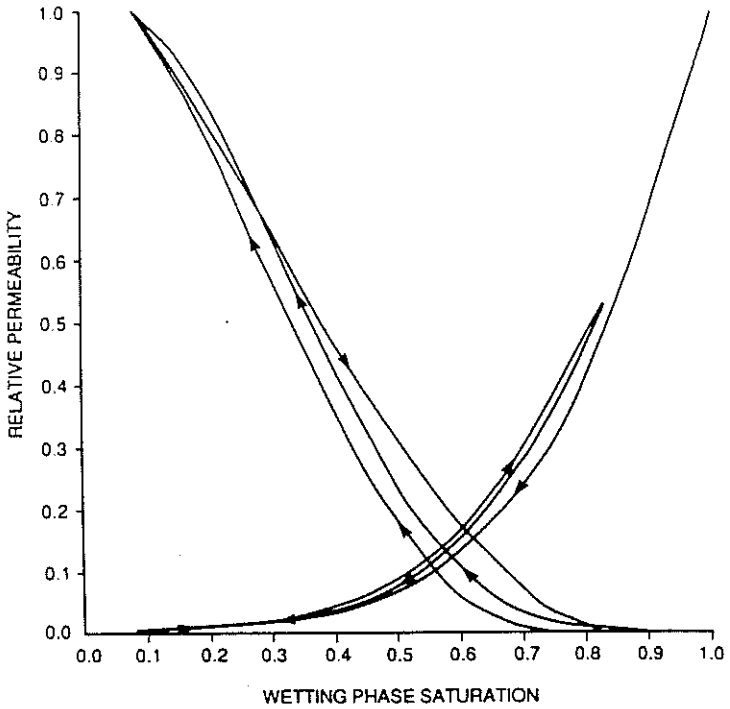

Fig. 22. Pore-level model predictions of hysteresis in relative permeability for low-aspect-ratio medium with type 4 correlation, note that wetting phase relative permeability is slightly larger in imbibition than in drainage.

permeability is smaller in cases where either the pore-body, or pore-throat, size distributions were narrowed.

It is apparent from both Figures 24 and 25 that in imbibition the nonwetting phase is trapped in the largest pores, because the trapped saturation is significantly larger for the base cases than it is in the cases with either narrow pore-body, or pore-throat size distribution. Narrowing the body-size is seen in Figure 25 to have a greater effect upon the residual saturation.

Figure 26 shows the effect of narrowing the pore-size distributions for the unconsolidated medium. The imbibition relative permeability of the nonwetting phase was slightly smaller in the case of a narrow pore-size distribution and significantly smaller in the case of narrow pore-throat size distribution. The other relative permeabilities were essentially unaffected. As in the consolidated media, the major impact on the relative permeability resulted from narrowing the pore-throat size distribution.

Consideration of the effects of pore-size distribution independent from all other effects is difficult. This problem can perhaps most easily be seen if the results for the uncorrelated consolidated medium are considered. Because this medium is

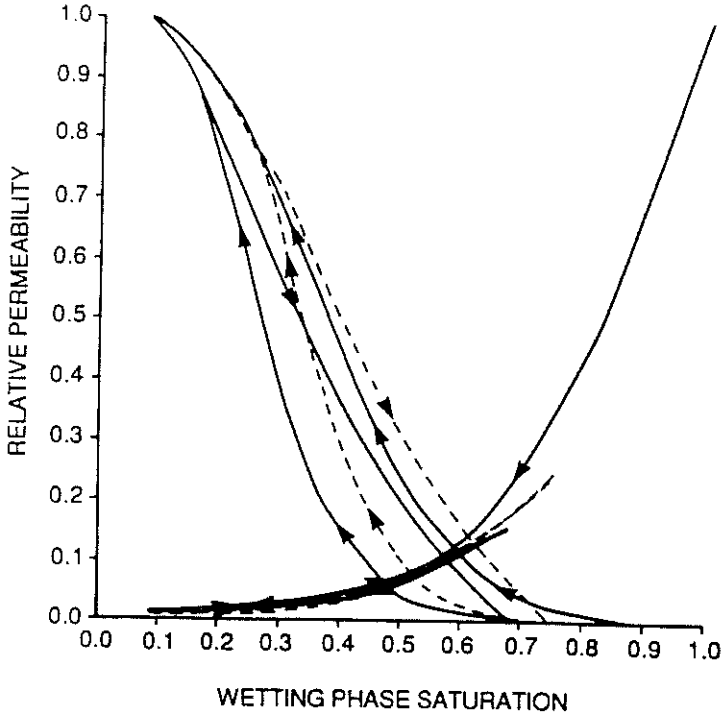

Fig. 23. Pore-level model predictions of hysteresis in relative permeability for low-aspect-ratio medium with type 8 correlation. Dashed line shows intermediate hysteresis loop.

uncorrelated, it is possible to characterize each of the four cases investigated (normal throat and body distributions, narrow throat distribution, narrow body distribution, and narrow throat and body distributions) with respect to the number of throats which are more likely to undergo retraction than choke-off, or vice versa. Since the throat and body sizes are independent (uncorrelated), calculation of an aspect ratio distribution is straightforward (see Appendix). The porous medium can then be characterized by the calculation of the fraction of throats which would undergo retraction before choke-off. It is important to recognize that this characterization describes the entire medium and does not equate to the likelihood of retraction versus choke-off, which is also impacted by the accessibility of the throats to nonwetting phase. The results of this calculation for the base-case distributions (consolidated medium) indicate that 17.1% of the throats would undergo retraction before choke-off. When the body-size distribution is narrowed, this percentage reduces to 11.5%. With normal body-sizes and a narrow throat-size distribution, the percentage reduces further to 4.2%. And with both distributions narrowed, all the throats will undergo choke-off before retraction. It should not be surprising, therefore that the results shown in Figure 24 follow the same ordering. Cases in which the distributions have been varied, while keeping the likelihood of choke-off versus retraction constant, have not been conducted.

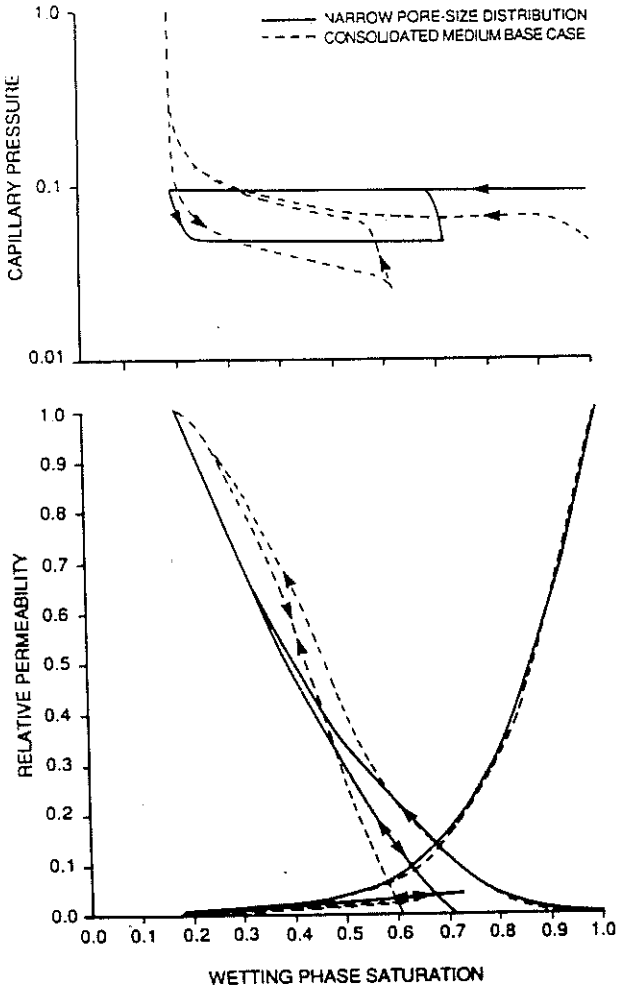

Fig. 24. Comparison of pore-level model predictions of hysteresis in relative permeability and capillary pressure of high aspect ratio porous media with very narrow and base case pore-throat distribution (type 6 correlation, throats correlated with bodies).

5. Conclusions

- Pore-level modeling is an effective tool for understanding the impact of pore structure in causing hysteresis behavior in steady-state relative permeability and capillary pressure in strongly-wetting systems at low capillary number.
- Pore-body to pore-throat aspect ratio is the most important structural determinant of the hysteresis behavior.
- The concept of bounding curves for relative permeability is invalid for porous media with intermediate aspect ratio.
- The structure of the backbone of the nonwetting phase is the primary determinant

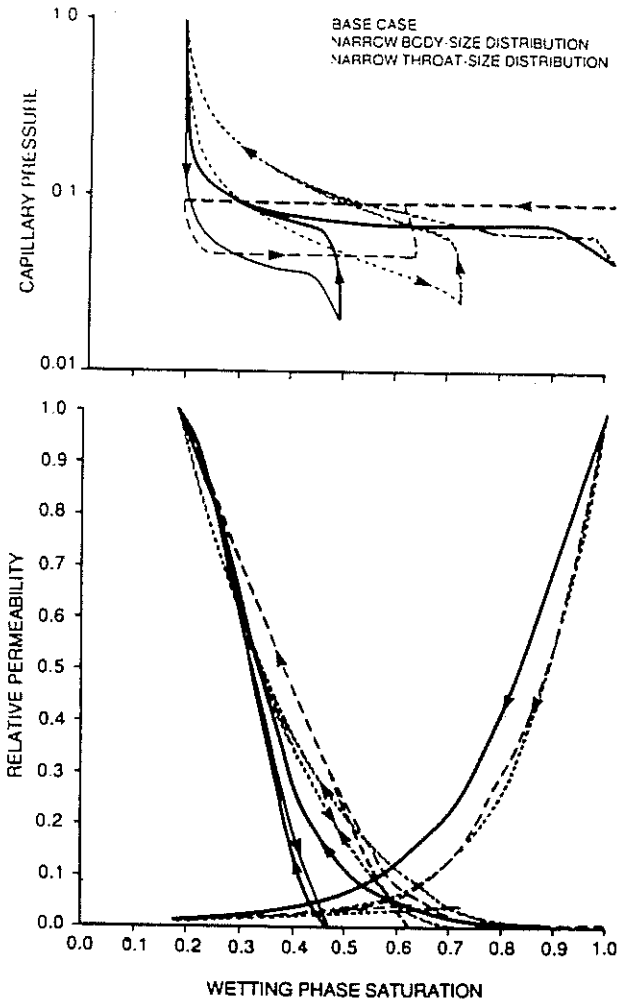

Fig. 25. Comparison of pore-level model predictions of hysteresis in relative permeability and capillary pressure of high-aspect-ratio porous media with very narrow and base case pore-size distributions (no correlation).

of its relative permeability. During imbibition this structure is, to a large extent, determined by the relative importance of choke-off and retraction, which is highly influenced by the aspect ratio of the medium. (Choke-off dominates in high aspect ratio media). The pore-size distribution is of secondary importance.

- In high-aspect-ratio media, typical of consolidated media, imbibition capillary pressure curves of strongly-wetting fluids do not give direct information about pore-body size because the primary mechanism in imbibition is choke-off which depends primarily upon pore-throat size.
- Spatial correlation between pore-throat sizes also impacts the nonwetting phase structure and, thereby, the shape of relative permeability curves. Increasing the

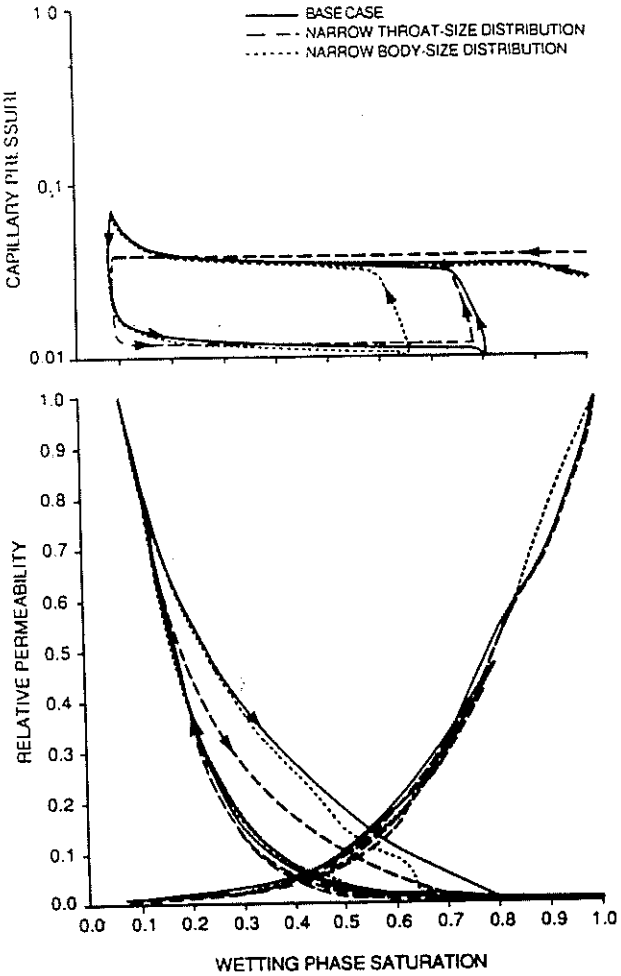

Fig. 26. Comparison of pore-level model predictions of hysteresis in relative permeability and capillary pressure of low-aspect-ratio porous media with very narrow and base case pore-size distributions (no correlation). Relative permeabilities for the cases in which both pore-throat and body sizes are narrowed is indistinguishable from those in which only throat size is narrowed.

extent of correlation between pore-throats increases the nonwetting phase relative permeability and slightly decreases the wetting phase relative permeability.

- Whereas we have explored many of the impacts of pore-structure upon relative permeability and capillary pressure, there are others which remain. Additionally, seldom is there enough experimental information describing the pore structure of any specific porous medium (particularly correlation between pore-sizes) to allow a priori calculation of relative permeability and capillary pressure with a high degree of certainty.

Appendix: Retraction Versus Choke-Off

In the section entitled PORE LEVEL EVENTS, the criteria for choke-off

$$2H = \frac{C}{r_t}$$

and retraction

$$2H = \frac{2}{r_b z_{nw}}$$

were given. If body-throat combinations are considered, the likelihood of retraction relative to choke-off is determined by

$$r_b \begin{cases} < \dfrac{2r_t}{Cz_{nw}} & \text{retraction preferred,} \\ = \dfrac{2r_t}{Cz_{nw}} & \text{choke-off and retraction equally likely,} \\ > \dfrac{2r_t}{Cz_{nw}} & \text{choke-off preferred.} \end{cases}$$

For uncorrelated systems, the probability that a throat has radius r_t and that a body has radius r_b is, simply, the product of the two individual probabilities

$$f_t(r_t) f_b(r_b).$$

If the individual body and throat-size distributions are normalized, such that

$$\int_0^\infty dr_t f_t(r_t) \int_0^\infty dr_b f_b(r_b) \equiv 1$$

then the fraction of throat-body pairs in which retraction is of equal, or greater, likelihood to occur relative to choke-off is given by

$$\int_0^\infty dr_t \int_0^{2r_t/Cz_{nw}} dr_b [f_t(r_t) \cdot f_b(r_b)]$$

For the throat- and body-size distributions of interest, these integrals were computed numerically.

Acknowledgments

The authors wish to thank Kishore Mohanty for his advice on pore-level modelling and Walt Ring for his help with the relative permeability measurements reported

here. We also thank Ron Giordano, Jake Rathmell, Fred Stalkup and Aaron Zick for their helpful review of this paper.

References

Adamson, A. W., 1982, *Physical Chemistry of Surfaces*, 4th edn, Wiley, New York.

Anderson, W. G., 1986a, Wettability literature survey–Part 1: Rock/oil/brine interactions, and the effects of core handling on wettability, *J. Pet. Tech.* (Oct) 1125–1144.

Anderson, W. G., 1986b, Wettability literature survey – Part 3: Wettability measurement, *J. Pet. Tech.* (Nov.), 1246–1262.

Anderson, W. G., 1986c, Wettability literature survey – Part 4: The effects of wettability on capillary pressure, *J. Pet. Tech.* (Dec.).

Anderson, W. G., 1987, Wettability literature survey – Part 5: The effects of wettability on relative permeability, *J. Pet. Tech.*

Aziz, A. and Settari, T., 1979, *Petroleum Reservoir Simulation*, Applied Science Publishers, London, pp. 396–401.

Batycky, J. P. and McCaffrey, F. G., 1978, Low interfacial tension displacement studies, paper #78–29–26, presented at the 29th Annual Meeting of Petroleum Society of CIM, Calgary, June 13–16.

Bacri, J. C., Leygnac, C., and Salin, D., 1985, Evidence of capillary hyperdiffusion in two-phase fluid flows, *J. Physique Lett.* **46,** L467–472.

Brown, W. O., 1957, The mobility of connate water during a water flood, *Trans. AIME* **210,** 190–195.

Chandler, R., Koplik, J., Lerman, K., and Willemsen, J. F., 1982, Capillary displacement and percolation in porous media, *J. Fluid Mech.* **119,** 249–267.

Chatzis, I., 1980, A network approach to analyze and model capillary and transport phenomena in porous media, PhD thesis, U. of Waterloo, Canada.

Chatzis, I. and Dullien, F. A. L., 1977, Modelling pore structure by 2-D and 3-D networks, with applications to sandstones, *JCPT* **16,** 97–108.

Chatzis, I. and Dullien, F. A. L., 1982, Application of the theory of percolation for a model of drainage in porous media and relative permeability of injected non-wetting liquid, *Rev. l'Institut Francais du Petrole* **37,** 183–205.

Chatzis, I. and Dullien, F. A. L., 1984, Dynamic immiscible displacement mechanisms in pore-doublets: Theory versus experiment, *J. Colloid Interface Sci.* **91,** 199–123.

Chatzis, I., Morrow, N. R., and Lim, H. T., 1983, Magnitude and detailed structure of residual oil saturation, *SPEJ*, April, 311–326.

Chen, J. and Koplik, J., 1985, Immiscible fluid displacement in small networks, *J. Colloid Interface Sci.* **108,** 304–330.

Cohen, M. H. and Lin C., 1981, *Proc. Conf. Macroscopic Properties of Disordered Media*, eds. R. Burridge, S. Childress, and G. Paapanicolau, Springer-Verlag, New York 74.

Colonna, J., Brissaud, F., and Millet, J. L., 1971, Evolution of capillary and relative permeability hysteresis, *SPEJ* 28–38.

Colonna, J. and Millet, J. L., 1970, Effect des deplacements diphasiques alternes sur les proprietes hydrodynamiques des Roches, *Rev. Inst. Francais Petrole*, Nov., 1317–1328.

Dagan, Z., Weinbaum, S., and Pfeffer, 1982, An infinite-series solution for the creeping motion through an orifice of finite length, *J. Fluid Mech.* **115,** 505–523.

Danis, M. and Jacquin, C., 1983, Influence du contraste de viscosites sur les permeabilites relatives lors du drainage: Experimentation et modelisation, *Rev. Inst. Francais Petrole* **38,** 723–733.

Diaz, C. E., Chatzis, I., and Dullien, F. A. L., 1987, Simulation of capillary pressure curves using bond correlated site percolation on a simple cubic network, *Transport in Porous Media* **2,** 215–240.

Dombrowski, H. S. and Brownell, L. E., 1954, Residual equilibrium saturation of porous media, *Ind. Eng. Chem.* **46,** 1207–1219.

Donaldson, E. C., Lorenz, P. B., and Thomas, R. D., 1966, The effects of viscosity and wettability on oil and water relative permeabilities, paper SPE 1562 presented at the 41st Annual Tech. Conf. of SPE, Dallas, TX, Oct. 2–5.

Dullien, F. A. L., 1979, *Porous Media: Fluid Transport and Pore Structure*, Academic Press, Ne York.

Dullien, F. A. L. and Dhawan, G. K., 1974, Characterization of pore structure by a combination o quantitative photomicrography and mercury porosimetry, *J. Colloid Interface Sci.* **47**, 337–349.

Dullien, F. A. L. and Dhawan, G. K., 1975, Bivariate pore-size distributions of some sandstones, *J Colloid Interface Sci.* **52**, 129–135.

Dullien, F. A. L., Lai, F. S. Y., and MacDonald, I. F., 1986, Hydraulic continuity of residual wettin phase in porous media, *J. Colloid Interface Sci.* **109**, 201–218.

Elman, H. C., 1982, Iterative methods for large, sparse, nonsymmetric systems of linear equations Research Report #229, Yale Univ. Dept. Comp. Sci.

Ehrlich, R. and Crane, F. E., 1969, A model for two-phase flow in consolidated materials, *SPEJ* **21**, 221–231.

Evrenos, A. I. and Corner, A. G., 1969, Numerical simulation of hysteretic flow in porous media, paper SPE 2693 presented at the 44th Annual Fall Meeting of SPE, Denver, Colo., Sept 28–Oct. 1.

Fatt, I., 1956a, The network model of porous media I. Capillary characteristics *Pet. Trans. AIME* **217**, 144–159.

Fatt, I., 1956b, The network model of porous media II. Dynamic properties of a single size tube network *Pet. Trans. AIME* **207**, 160–163.

Fatt, I., 1956c, The network model of porous media III. Dynamic properties of networks with tube radius distribution, *Pet. Trans. AIME* **207**, 164–181.

Fulcher, R. A. Jr, Ertekin, T., and Stahl, C. D., 1985, Effect of capillary number and its constituents on two-phase relative permeabilities, *SPEJ*, Feb., 249–260.

Geffen, T. M., Owens, W. W., Parrish, D. R., and Morse, 1951, Experimental investigation of factors affecting laboratory relative permeability measurements, *Pet. Trans. AIME* **192**, 99–110.

Gladfelter, R. E. and Gupta, S. P., 1978, Effect of fractional flow hysteresis on recovery of tertiary oil, paper SPE 7577 presented at the 53rd Annual Fall Technical Conf. and Exhibition of SPE, Houston, TX, October 1–3.

Goddard, R. R., Gardner, G. H. F., and Wyllie, M. R. J., 1962, Some aspects of multi-phase distribution in porous bodies, *Proc. Symp. Interactions Between Fluids and Particles*, Inst. Chem. Eng., London, June 20–22, pp. 326–332.

Heiba, A. A., Sahimi, M., Davis, H. T., and Scriven, L. E., 1982, Percolation theory of two-phase relative permeability, SPE 11015, presented at the 57th annual Fall Meeting of the Society of Petroleum Engineers, New Orleans, LA.

Hopkins, M. R. and Ng, K. M., 1986, Liquid-liquid relative permeability: network models and experiments, *Chem. Eng. Commun.* **46**, 253–279.

Hulin, J. P., Chairlaix, E., Plona, T. J., Oger, L., and Guyon, E., 1987, Experimental study of tracer dispersion in sintered glass beads with a bidisperse size distribution, preprint submitted to AIChE.

Jerauld, G. R., Hatfield, J. C., Scriven, L. E., and Davis, H. T., 1984, Percolation and conduction on Voronoi and triangular networks: a case study in topological disorder, *J. Phys. C: Solid State Phys.* **17**, 1519–1529.

Jerauld, G. R., Scriven, L. E., and Davis, H. T., 1984, Percolation and conduction on the 3D Voronoi and regular networks: a second case study in topological disorder, *J. Phys. C: Solid State Phys.* **17**, 3429–3439.

Katz, A. J. and Thompson, A. H., 1987, Prediction of rock electrical conductivity from mercury injection measurements, *J. Geophys. Res.* **92**, 599–607.

Katz, A. J. and Thompson, A. H., 1987, Quantitative prediction of permeability in porous rocks, *Phys. Rev. B* **34**, 8179–8181.

Keelan, D. K. and Pugh, V. J., 1975, Trapped-gas saturations in carbonate formations, *SPEJ*, April, 149–160.

Killough, J. E., 1976, Reservoir simulation with history-dependent saturation functions, *SPEJ*, February, 37–48.

Kirkpatrick, S., 1973, Percolation and conduction, *Rev. Mod. Phys.* **45**, 574–588.

Koplik, J., 1982, Creeping flow in two-dimensional networks, *J. Fluid Mech.* **119**, 219–247.

Koplik, J., Lin, C., and Vermette M., 1984, Conductivity and permeability from microgeometry, *J. Appl. Phys.* **56**, 3127–3131.

Koplik, J., Wilkinson, D., and Willemsen, J. F., 1983, Percolation and capillary fluid displacement, *Proc. Workshop on Mathematics and Physics of Disordered Media: Percolation, Random Walk, Modeling and Simulation*, ed. B. D. Hughes and B. W. Ninham, held in Minneapolis, MN, Feb. 13–19, Lecture Notes in Mathematics No. **1035**, Springer-Verlag, New York.

Labastie, A., Guy, M., Delclaud, J. P., and Iffly, R., 1980, Effect of flow rate and wettability on water-oil relative permeabilities and capillary pressure, SPE 9236 presented at the 55th Tech. Conf. at SPE-AIME, Dallas, TX, Sept. 21–24.

Land, C. S., 1968, Calculation of imbibition relative permeability for two- and three-phase flow from rock properties, *SPEJ*, June, 149–156.

Larson, R. G., 1981, Derivation of generalized Darcy equations for creeping flow in porous media, *I&EC Fundamentals* **20**, 132–137.

Larson, R. G., Scriven, L. E., and Davis, H. T., 1981, Percolation theory of two-phase flow in porous media, *Chem. Eng. Sci.* **36**, 57–73.

Lenormand, R., Zarcone, C., and Sarr, A. J., 1983, Mechanisms of the displacement of one fluid by another in a network of capillary ducts, *J. Fluid Mech.* **135**, 337–353.

Lenormand, R. and Zarcone, C., 1984, Role of roughness and edges during imbibition in square capillaries, paper SPE 13264 presented at the 59th Annual Technical Conference and Exhibition of SPE, Houston, TX, Sept. 16–19.

Leverett, M. C., 1938, Flow of oil-water mixtures through unconsolidated sands, *Trans. AIME* **132**, 149–171.

Levine, S. and Cuthiell, D. L., 1986, Relative permeabilities in two-phase flow through porous media: an application of effective medium theory, *J. Can. Petr. Tech.*, Sept-Oct., 74–84.

Li, Y., Laidlaw, W. G. and Wardlaw, N. C., 1986, Sensitivity of drainage and imbibition to pore structures as revealed by computer simulation of displacement process, *Adv. Colloid Interface Sci.* **26**, 1–68.

Li, Y. and Wardlaw, N. C., 1985, 'The influence of wettability and critical pore throat size on snap-off, *J. Colloid Interface Sci.* **109**, 461–472.

Li, Y. and Wardlaw, N. C., 1985, Mechanisms of nonwetting phase trapping during imbibition at slow rates, *J. Colloid Interface Sci.* **109**, 473–486.

Lin, C. and Cohen, M. H., 1982, Quantitative methods for microgeometric modeling, *J. Appl. Phys.* **53**, 4152–415.

MacDonald, I. F., Kaufmann, P., and Dullien, F. A. L., 1986, Quantitative image analysis of finite porous media: II. Specific genus of cubic lattice models and Berea sandstone, *J. Microsc.* **144**, 297–316.

Mathers, E. G. and Dawe, R. A., 1985, Visualization of microscopic displacement processes within porous media in EOR capillary pressure effects, *Proc. ACTES, 3rd, European Meeting On Improved Oil Recovery* **1**, 49–58.

Mattax, C. C. and Kyte, J. R., 1961, Ever see a water flood? *Oil and Gas J.* **59**, 115.

Meijering, J. L., 1953, Interface area, edge length and number of vertices in crystal aggregates with random nucleation, *Philips Res. Rep.* **8**, 270–90.

Meyers, K. O. and Salter, S. J., 1984, Concepts pertaining to reservior pretreatment for chemical flooding, paper SPE/DOE 12696 presented at the fourth Symposium on Enhanced Oil Recovery, Tulsa, OK, April 15–18.

Mohanty, K. K., 1981, Fluids in Porous Media: Two-Phase Distribution and Flow, PhD thesis, University of Minnesota, Minneapolis.

Mohanty, K. K., Davis, H. T., and Scriven, L. E., 1987, Physics of oil entrapment in water-wet rock, *SPE Reservoir Engineering* **1**, 113–127.

Mohanty, K. K. and Salter, S. J., 1982, Multiphase flow in porous media: II Pore-level modeling, SPE 11018 presented at the 57th Tech. Conf. at SPE-AIME, New Orleans, Sept. 26–29.

Moore, T. F. and Slobod, R. L., 1956, The effect of viscosity and capillarity on the displacement of oil by water, *Prod. Monthly* **20**, 20–30.

Morgan, J. T. and Gordon, D. T., 1970, Influence of pore geometry on water-oil relative permeability, *J. Petrol. Tech.* **22**, 1199.

Morrow, N. R., 1970, Irreducible wetting-phase saturations in porous media, *Chem. Eng. Sci.* **25**, 1799–1815.

Muskat, M., Wyckoff, R. D., Botset, H. G. and Meres, M. W., 1937, 'Flow of gas-liquid mixtures through sands, *Trans. AIME* **123**, 69–96.

Naar, J., Wygal, R. J., and Henderson, J. H., 1962, Imbibition relative permeability in unconsolidated porous media, *SPEJ* **2**, 13–17.

Osoba, J. S., Richardson, J. G., Kerver, J. K., Hafford, J. A., and Blair, P. M., 1951, Laboratory measurements of relative permeability, *Pet. Trans. AIME* **191**, 47–56.

Owens, W. W. and Archer, D. L., 1971, The effect of rock wettability on oil-water relative permeability relationships, *J. Pet. Tech.* **23**, 873–878.

Payatakes, A. C., Ng, K. M., and Flummerfelt, R. W., 1980, Oil ganglion dynamics during immiscible displacement: model formulation, *AIChE J.* **26**, 430.

Pickell, J. J., Swanson, B. F. and Hickman, W. B., 1966, Application of air-mercury and oil-air capillary pressure data in the study of pore structure and fluid distribution, *SPEJ* **6**, 55–61.

Poulovassilis, A., 1970, Hysteresis of pore water in granular porous bodies, *Soil Science* **109**, 5–12.

Ramakrishnan, T. S. and Wasan, D. T., 1986, Effect of capillary number on the relative permeability function for two-phase flow in porous media, *Powder Technol.* **48**, 99–124.

Ramondi, P. and Torcaso, M. A., 1964, Distribution of the oil phase obtained upon imbibition of water, *SPEJ* **4**, March, 49–54.

Richardson, J. G., Kerver, J. K., Hafford, J. A., and Osoba, J. S., 1952, Laboratory determination of relative permeability, *Pet. Trans. AIME* **195**, 187–196.

Roof, J. G. 1970, Snap-off of oil droplets in water-wet pores, *SPEJ* **10**, March, 85–90.

Russell, R. G., Morgan, F., and Muskat, M., 1947, Some experiments on the mobility of interstitial waters, *Trans. AIME* **170**, 51–61.

Ruzyla, K., 1986, Characterization of pore space by quantitative image analysis, *SPE Formation Evaluation*, August, 389–398.

Salter, S. J. and Mohanty, K. K., 1982, Multiphase flow in porous media: I. Macroscopic observations and modeling, SPE 11017 presented at the 57th Annual Tech. Conf. of the SPE-AIME, New Orleans, Sept. 26–29.

Sandberg, C. R., Gournay, L. S., and Sipple, R. F., 1958, The effect of fluid-flow rate and viscosity on laboratory determinations of oil-water relative permeabilities, *Trans. AIME* **213**, 36–43.

Schultz, M. H. *et al.*, 1983, *Conjugate Gradient-Like Iterative Methods Project Two-Year Summary*, Scientific Computing Associates.

Talash, A. W., 1976, Experimental and calculated relative permeability data for systems containing tension additives, paper SPE 5810 presented at the Symposium on Improved Oil Recovery, Tulsa, OK, March 22–24.

Talsma, T., 1970, Hysteresis in two sands and the independent domain model, *Water Resour. Res.* **6**, 964–970.

Topp, G. C. and Miller, E. E., 1966, Hysteretic moisture characteristics and hydraulic conductivities for glass-bead media, *Soil Sci. Soc. Am. Proc.* **30**, 156.

Voronoi, G., 1908, Nouvelles appillications des paramèteres continus à la théorie des formes quadratiques, *J. Reine Angew. Math.* **134**, 198–287.

Wardlaw, N. C. and Taylor, R. P., 1976, Mercury capillary pressure curves and the interpretation of pore-structure and capillary behavior in reservoir rocks, *Bull. Canadian Petroleum Geology* **24**, 225–262.

Wilkinson, D., 1986, Percolation effects in immiscible displacement, *Phys. Rev. A.* **34**, 1380–1391.

Wilkinson, D. and Willemsen, J. F., 1983, Invasion percolation: a new form of percolation theory, *J. Phys. A.: Math. Gen.* **16**, 3365–3376.

Winterfeld, P. H., 1981, Percolation and Conduction Phenomena in Disordered Composite Media, PhD thesis, University of Minnesota, Minneapolis.

Yadav, G. D., Dullen, F. A. L., Chatzis, I., and MacDonald, I. F., 1987, Microscopic distribution of wetting and nonwetting phases in sandstones during immiscible displacements, *SPE Reservoir Engineering*, **2**, 137–147.

Yanuka, M., Dullien, F. A. L., and Elrick, D. E., 1984, Serial sectioning digitization of porous media for two- and three-dimensional analysis and reconstruction, *J. Microsc.* **135**, 159–168.

Yanuka, M., Dullien, F. A. L., and Elrick, D. E., 1986, Percolation processes and porous media: I.

Geometrical and topological model of porous media using a three-dimensional joint pore size distribution, *J. Colloid Interface Sci.* **112**, 24–41.

Yuan, H. H., 1981, The influence of pore coordination on petrophysical parameters, paper SPE 10074 presented at the 56th Annual Technical Conference of the SPE, San Antonio, TX, Oct. 5–7.

Yuster, S. T., 1951, Theoretical considerations of multiphase flow in idealized capillary systems, Proc. 3rd World Petroleum Congress, The Hague, Netherlands, Section II, pp. 437–445.